國立交通大學

光電工程研究所碩士班

碩 士 論 文

複合多波段發光二極體混光平台之建構

Platform of Optimized Additive Mixing via Multi-color LEDs

研 究 生：董雨隴

指導教授：田仲豪 博士

中 華 民 國 九 十 八 年 七 月

複合多波段發光二極體混光平台之建構

Platform of Optimized Additive Mixing via Multi-color LEDs

研 究 生：董雨隴　　Student：Yu-Lung Tung

指導教授：田仲豪　　Advisor：Chung-Hao Tien

國 立 交 通 大 學

光電工程研究所碩士班

碩 士 論 文

A Thesis

Submitted to Department of Photonics

College of Electrical and Computer Engineering

National Chiao Tung University

in partial Fulfillment of the Requirements

for the Degree of

Master

in

Department of Photonics

July 2009

Hsinchu, Taiwan, Republic of China

中華民國九十八年七月

複合多波段發光二極體混光平台之建構

學生：董雨隴　　指導教授：田仲豪

國立交通大學光電工程學系碩士班

摘　　要

自從 1906 年第一顆發光二極體(Light Emitting Diode, LED)被發明出來，經過了 90 年的發展，直到日本的日亞化學(Nichia)在 1996 年發表高亮度的藍光和白光 LED 技術，LED 才被視為俱有潛力成為新一代的照明光源。然而，LED 是窄頻的光源，和傳統的廣頻譜光源相比，在許多特性上有很大的差異。其中最大的差異，在於頻譜的變動特性，傳統的燈源，最多只具有調整亮度的功能，無法在頻譜特性上做調整。而 LED 卻能夠藉由不同的組合，在某些情況下達到相同的效果，這在色彩學上稱為同色異譜(Metamerism)的概念。

因而此研究的主題，主要由以往照明頻譜的特性參數上著手，嘗試建立一個軟體平台，用來挑選適當的 LED 組合，以得到最佳的混光頻譜。接著實際建構一個多波段 LED 的混光系統，並希望能夠將模擬與實際系統的結果成功的連結起來。

Platform of Optimized Additive Mixing via Multi-color LEDs

Student：Yu-Lung Tung **Advisors：Dr. Chung-Hao Tien**

Department of Photonics
National Chiao Tung University

ABSTRACT

Ninety years after the first LED was invested in 1906, Nichia developed high intensity blue and white light LEDs in 1996. Only until then are LEDs thought to be the lighting sources of next generation. However, unlike the general lighting sources, LEDs have very narrow band-width spectrum. Thus, LEDs have the flexibility on synthesizing different spectra with the same properties, which is called “Metamerism” in color science.

This thesis focused on the combinations of LEDs to fulfill the general lighting parameters. We first developed a MatLab based GUI simulation tool to calculate the optimized LED spectrum. We then designed and fabricated a LED matrix to verify the simulation results, and expected to synchronize the practical LED clusters with the program.

致謝

首先要感謝我指導教授田仲豪老師這幾年來在研究上、表達能力及生活細節上無私的細心指導，並且提供我良好的研究環境與資源，使我在碩士生涯對於色彩學與照明規範有了深入的了解，並順利完成本論文。

實驗室的日子裡，首先要感謝簡銘進學長、陳筱儒學妹和林至宏學弟在研究過程提供許多寶貴的建議與幫助，還有鄭璧如學姊、陸彥行、洪健翔、藍子翔、鍾積賢學長在研究過程提供許多寶貴的建議，同時還要感謝鄭榮安博士和其他學長姊、同學、學弟妹以及助理古明嬿小姐在課業上、生活上、研究上的幫助與分享，並陪伴我一起度過這些快樂的日子。

此外，我要感謝永捷科技李應利經理和張國輝經理，在研究期間提供我硬體技術及系統開發上的協助，讓我實驗得以順利完成。

另外，我也要感謝陳皇銘教授、趙昌博教授、陳政寰教授對於我研究所給予的寶貴建議與指教。

最後，對於我的父母、姐姐以及女友蘇怡樺，我要感謝你們多年來的支持與鼓勵，還有生活上的細心照顧與關懷，使我能夠無後顧之憂的研究與學習，並順利完成碩士學業。這份喜悅我將與幫助過我的各位分享。

Table of Contents

Figure Captions

Tables

Chapter 1

Introduction

Ninety years after the first LED was invested in 1906, Nichia developed high intensity blue and white light LEDs in 1996. Only until then are LEDs thought to be the lighting sources of next generation. However, unlike the general lighting sources, LEDs have relatively narrow band-width spectrum, and are still far away to fulfill the general lighting criteria. Thus, this research is focused on improving the lighting quality of LED spectrum, expecting to create the LED light source that can fulfill the general light source requirements.

1.1 Introduction of the LED

1.1.1 Emergence of the LED

LED was first invented by Henry Joseph Round in 1906, and the technology was silence for the next ninety years. In this period, the most popular application for LED was used as the circuit indicator. However, thanks to the flourish developments of the semiconductor industry, new materials were found, and many researchers were devoted to improve the p-n junction injection, the light extraction ability, and the fabrication process. In 1990s, Nakamura and other researchers had great improvements in the InGaN LED technology, and successfully demonstrated the first high efficiency blue LED. After that, the high brightness white LED can be achieved by mixing the blue LED with yellow phosphor, and this launched the emergence of the LED. Besides, the luminous efficiency of primary color LEDs, such as green, red, and yellow, were also strongly improved in this period [Fig. 1.1].

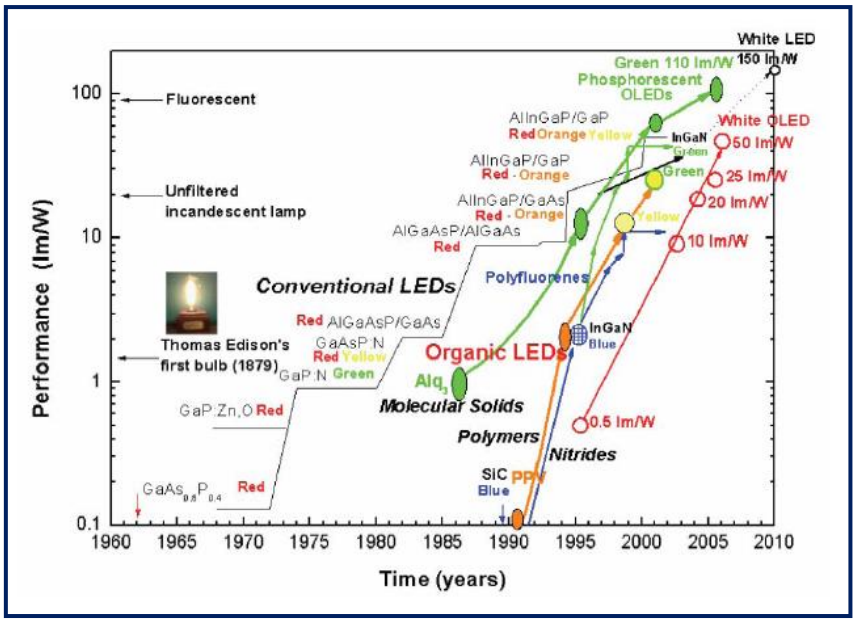

Fig. 1.1 Luminous efficiency improvement in LED via Si and organic base

Thus, accompanying with the rising tide of mobile phone, LED had found the specific application in keypad and monitor backlight. This market brought the fuel for the growth of LED industry [Fig. 1.2], and still takes half of the revenue nowadays [Fig. 1.3] [1].

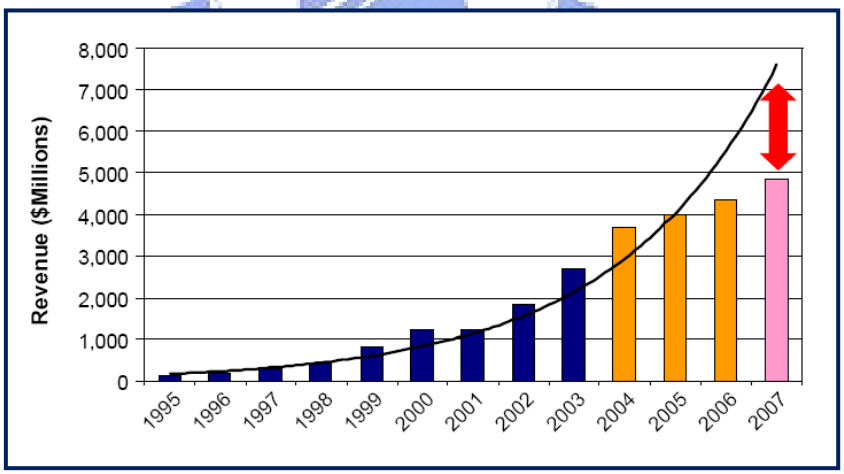

Fig. 1.2 Revenue growth of LED industry

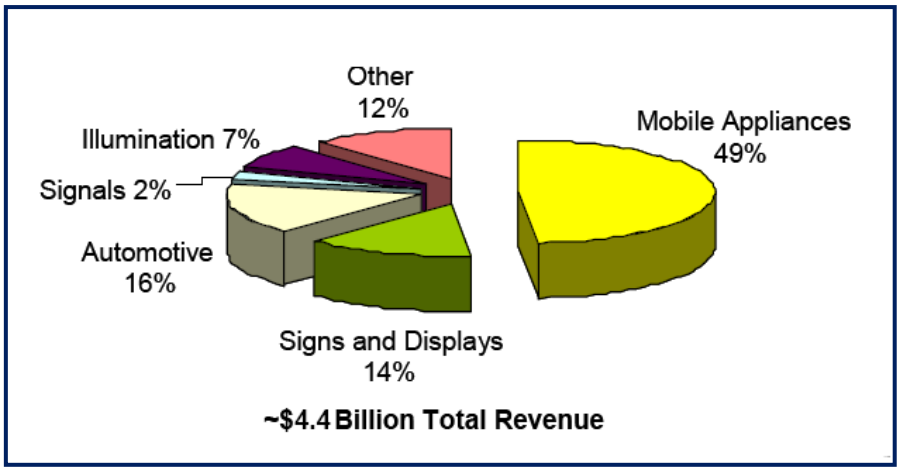

Fig. 1.3 Market segments of LED industry at 2006

However, the dominant mobile application is seemed to be saturated after 2006, and the growth of the industry is expected to be led by the display backlight, the automotive industry, and the illumination applications. Although the illumination application only take little share in the whole industry now, it is forecasted that the illumination will finally play an major role up to quarter market share in the future [Fig. 1.4].

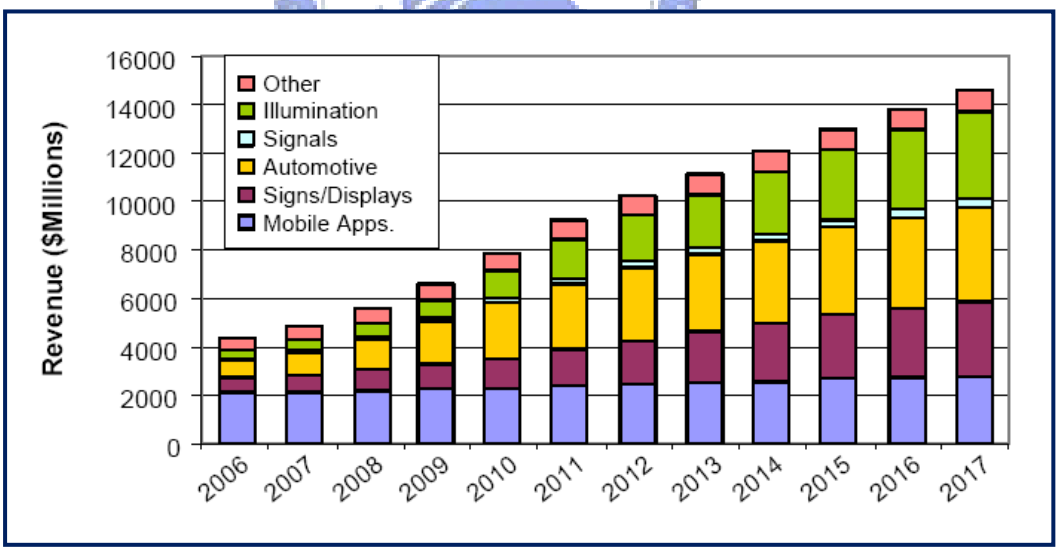

Fig. 1.4 Forecast of the LED market segments

1.1.2 Lighting properties of the LED

White light is the most general color used for general lighting application. Generally speaking, LED can generate the white light by three methods, multi-color LED mixing, UV LED with RGB phosphor, and blue LED with yellow phosphor [Fig.

1.5] [2]. Every approach has their pros and cons. For example, the multi-color LED mixing method can provide various and flexible light source color and high color rendering performance. However, the system also needs complex control circuit to maintain the color stability. Besides, the optical uniformity of mixing color should also be considered and well designed. The UV LED plus RGB phosphor method is the easiest way for commercialization thanks for the matured UV phosphor developments. Furthermore, the color stability of this type white light LED is the best, due to the reason that all the visible light generates from the same UV source. However, the luminous efficiency of the UV LED is still low and under developing. Besides, the penetrating UV light will cause some health issues of the human body. The last method uses the blue LED combines with the yellow phosphor. This is actually the most well-known and popular white light LED. The advantages of this method including the mature technology in high efficiency blue LED, easy fabrication process, and simple operation design. However, the color rendering property of this white light is about 70, which is not acceptable for general applications, and the white point of the LED may slightly drift during the operation.

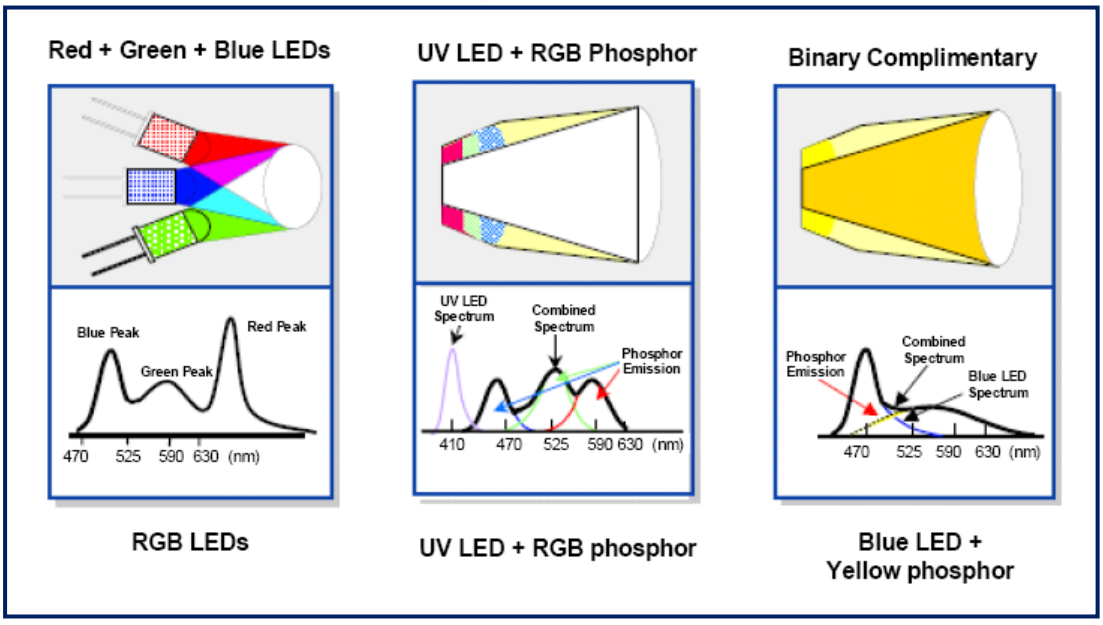

Fig. 1.5 Approaches for generating white light from LEDs

CCT value is the most common parameter used to describe the white point of the light source. Roughly speaking, high CCT value means the bluish white, and gives people calm and cool feeling. On the other side, low CCT value stands for reddish white, and provides people much warm feeling. The sunlight is usually has CCT value from 4000K~7500K. And the general commercial light sources, such as fluorescent lamp, incandescent bulb, and tungsten lamp, have the CCT value between 3000K~7000k. There have some interesting researches done to discuss about the human feeling and the light source CCT value. From a statistic result of the American families [3], it shows that the north residents love to choice lower CCT lamps whereas the south families prefer higher CCT ones. Besides, other research also founded out that people will feel reddish or yellowish of the object color if use the low CCT lamp in daytime, and will be better if change to use the high CCT lamp. On the opposite, people will feel weird when using high CCT lamp at nighttime, and much comfortable if choice the low CCT source. Thus, from the results, having a light source with tunable CCT value might be a good thing for general light source.

Besides the light source color, the color performance of the object under illuminant is also an important issue. The most popular parameter used is the CRI value. In the lighting guideline, the light source should have CRI higher than 70 for public lighting application, such as park, parking lot, and street light. And the CRI value should higher than 80 for general application. Besides, some specific application, such as jewelry story or gallery, might have more severe requirement, for example, CRI value higher than 90 or 95 [4]. The common light sources in the past are all have great color rendering ability. For example, incandescent bulb with CRI value 100, fluorescent lamp with CRI value higher than 85. Although the high intensity discharge lamps (HID) have lower CRI value, about 65-80, but as mentioned

before, this lamp is used for the outdoor lighting, and the luminous efficiency and high intensity are more concerned issue.

One of the biggest merits of LED is the tremendous long lifetime. The lifetime is defined as the time that needed for a light source to have 50% degradation of initial lumen output. Typically speaking, the lamp type LED has lifetime more than 6,000 hours, and the high power LED is more than 50,000 hours. Both are much longer than the incandescent lamp, which has lifetime less than 1,500 hours [Fig. 1.6] [5]. Besides, the luminous efficiency of the LED, generally 60lm/W, is much higher than the luminous efficiency of incandescent lamp, usually 15lm/W. Thus, in the point source application, it is well believed that the LED will finally substitute the incandescent lamp.

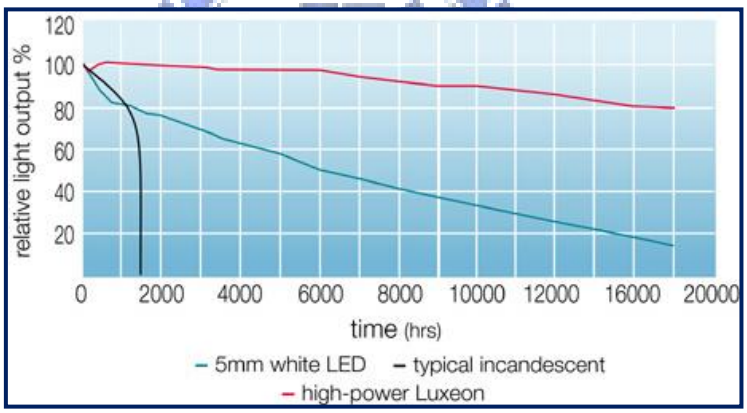

Fig. 1.6 Lifetime of lamp LED (blue), high power LED (red)
, and incandescent lamp (black)

The light intensity of indoor lighting is set between 200lx to 500lx. And the light intensity of the store or the display window is set between 1000lx to 2000lx [4]. However, those values are just for general case, and may modify by the application situation. For example, due to the reason that the human visual system will retrograde as time pass. Thus, children have much accuracy vision, and the luminous intensity may use lower value than the standard [3]. On the opposite, the luminary designed for elder usage might increase the intensity little higher than general case. In the past,

LED can only be operated under low electrical power, and provide low intensity light. This limited the application field of LED. However, the high power LED was developed to solve the problem, and it can provide really high intensity light with high luminous efficiency. This progress opened the automotive and general lighting field of the LED. Besides, the light emit only from the front side of the LED chip, which is different than the random direction radiation of the traditional light source. Thus, in the luminaire design, the directional light property of the LED may have less loss. For example, there have two light sources, one is HID lamp with luminous efficiency 100lm/W, and the other is LED with luminous efficiency 50lm/W. From the aspect of light source efficiency, the HID lamp is better than the LED. However, after considering the luminous efficiency of the luminaire, the LED will have higher overall luminous efficiency than the HID lamp. This is due to the reason that less light is trapped in the luminaire of the LED [Fig. 1.7].

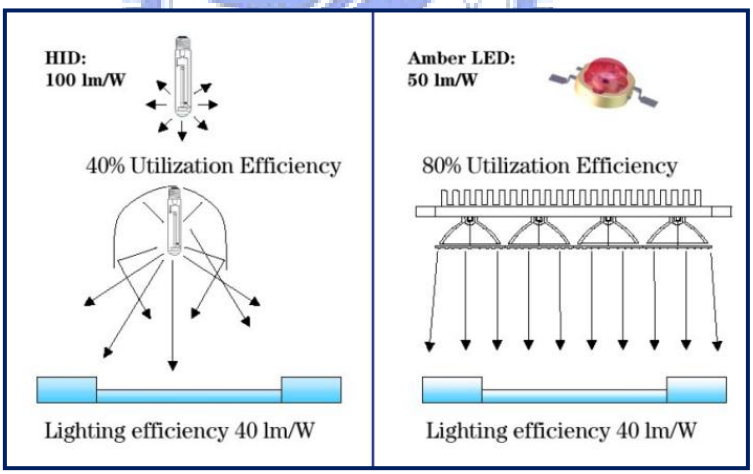

Fig. 1.7 Consideration of overall luminous efficiency

1.2 Introduction of the thesis

1.2.1 Motivation and Objective

As the properties aforementioned, LED, have the potential to be applied as the next generation light source. However, before penetrating into the general lighting market, many issues, such as the color rendering ability, color binning, heat management, luminous efficiency, and system stability, need to be considered. Many

companies and research institutes dedicate to solve the problems. In our research, we expect to study the lighting quality of the LED lighting system.

Light quality of a light source is complicate to be evaluated. Roughly speaking, it can be divided into two parts, subjective feelings and objective factors. Subjective feelings rely on a lot of human factor experiments and statistic data. In the past, some researches had been done to discuss the relationship between lighting intensity and work performance [6] [7] [8]. The other research is discussed about the relationship between moving object sensitivity and the roadway light source spectrum distribution [3]. All the researches are implemented under accurate research control factors and experimental setups. However, the experimental results are seemed to be ambiguous. On the other hand, some objective factors used in the traditional light sources are much more precise and solid. The factors include the color of the light source (CCT value), the color rendering performance (CRI value), and the power efficiency. Thus, our research will focused on the previous two color factors in LED lighting.

The semi-monochromatic spectrum property gives LED a chance to have various combinations. This spectrum flexibility is the most different part of the LED and the traditional light source. Combining the right set of LEDs with right ratios is not an easy question, and it will be too tedious to calculate by hand. Thus, the objective of the thesis is developing a GUI program for the multi-color LED mixing. The program is expected to provide the best mixing ratio, which fulfilling the CCT value imported by user and with maximum CRI value, for a given set of LEDs. After developing of the program, we will design a LED matrix to verify the calculating results and modify the calculating process.

1.2.2 Relative researches about spectrum optimization

Our goal is to find out the best mixing ratio of the LEDs. Thus, here are some articles mentioned about the optimization of the CRI values and luminance efficiency

in the past. In 2002, Neil Holger White Eklund used the genetic algorithm (GA) to optimize the luminance efficacy and CRI value for a spectrum power distribution (SPD) with specific chromaticity [9]. In the thesis, the author found out that the target objective genetic algorithm (TOGA) is better in calculating efficiency than GA for optimization the SPD. Besides, he also applied the algorithm to design the filters for the sulphur lamp, which has high luminous efficiency, about 100lm/W, low CRI value, about 78, and greenish-white apparent color. After adding the filters, the sulphur lamp was claimed to have CCT values 4000K or 4500K, CRI values 70 or 80, respectively, with the luminous efficacy still around 80lm/W. Thus, this method is a great solution for some high efficiency but low lighting quality lamps, such as sulphur lamps, metal halide lamps, and sodium vapor lamps, because by designing the appropriate filters, these lamps can improve their lighting quality with small sacrifice in luminous efficiency. However, using a filter to change the SPD of lighting sources is not practical, due to the high price in coating filters. Besides, the general fluorescent lamps nowadays also have luminous efficiency over 80lm/W with cheap price.

In the same time, Arturas Zukauskas, Feliksas Ivanauskas, Rimantas Vaicekauskas, Michael S. Shur, and Remis Gaska published a conference paper about the optimization of white light with multichip LEDs [10]. Based on the concept, they also published a series articles in this topics [11] [12] [13]. The core concept in their research was introduced an objective function

$$F(\lambda_1, \dots, \lambda_n, I_1, \dots, I_n) = \alpha K + (1-\alpha)R_a \qquad \text{(Eq. 3.1)}$$

Where α is the weighting that control the trade-off between the efficacy and the CRI value, $0 \leqq \alpha \leqq 1$. Therefore, the optimized profile was received by changing α value and scanning all combinations of the primary LEDs in visible wavelength range.

By their simulation results, the best dichromatic LED lamps seem to be useless. Although it have the highest luminous efficacy, the CRI values are all lower than 20. Besides, with the same luminous efficacy, the trichromatic combinations seem to have higher CRI values than the dichromatic combinations. Thus, the trichromatic LED lamps have the best performance of the luminous efficacy when the required CRI values are lower than 85. Furthermore, the simulation results show that the quadrichromatic combinations will be the best choices when expected CRI values are higher than 85 and lower than 97, and the quintichromatic combinations should be selected for required CRI values higher than 97.

Generally speaking, this research gave a great roadmap for the combination of primary LEDs. Due to the simulation results, the primary wavelengths and the number of LEDs were given to get the best performance in both CRI values and luminous efficacy. However, some practical details are not considered in the simulation. For example, the overall luminance efficiency is composed by many aspects, such as the device efficiency, which is determined by the material that used, the transmittance efficiency or the reflectance efficiency of the optical system, and the luminance efficiency that perceived by human visual system. All above parameters are relative to the wavelengths. Therefore, only considering the luminance efficacy is not complicated, and may not performed the best performance in a real world system.

After all, due to the reasons mentioned above, we decided to establish a simulation tool that is much more simple than the above two methods. Thus, in our method, we only consider to calculate the mix ratio of the given LEDs to get the best CRI values. We do not take the efficacy and the optimization SPD into consideration, due to the reason that both are not practical. Therefore, the objection of the thesis is to build a program as a tool for the sophisticated mixing calculation, and present the best mixing recipe for the further application. The parameters used for the calculation are

CCT value and CRI value, which are two most common and well-used standards in the world.

1.2.3 Organization of the thesis

In the following thesis, basic concepts and terminologies of the human vision and the color science will be described in the chapter 2. After that, the simulation flowchart and result will be given in the chapter 3. And finally, the specification of designed LED matrix and the experimental results will be obtained in the chapter 4. Finally, the conclusions and the future work will be mentioned in chapter 5.

Chapter 2

Foundations in Lighting

Visible light is simply a very small part of the electromagnetic spectrum that can be received by human visual system. In the thesis, we are studying the lighting quality of the LED, especially focusing on its unique SPD characteristic. Thus, realizing the mechanism that how does human percept the light is an important issue. Therefore, in the chapter, the basic concepts of the human vision and the fundamental models of the color science will be described.

2.1 Vision

2.1.1 Human visual system

Human visual system can be regarded as photo-detectors with different spectrum filters. The receptor cells of human eyes can be functionally divided into two kinds. They are called rods and cones based on their cell shapes. Rod is very sensitive to the light intensity, and help people to tell the darkness or brightness in the darkness environments. On the other hand, cone can only work under bright circumstance, and it helps people to perceive the color information of the outside world. Thus, human eyes can receive color and brightness information in the bright environments, and only brightness information under the dark surroundings.

Generally speaking, each human eye has about hundred million rods and seven million cones. However, Rods and cones distribute a little different on the retina [Fig. 2.1]. About 100,000~150,000 cones are concentrated in the vicinity of the optical axis in the fovea centralis, which is the highest resolution part of the eye [14]. On the opposite, the rods are rarely found at fovea centralis, but distribute much widely over the whole retina.

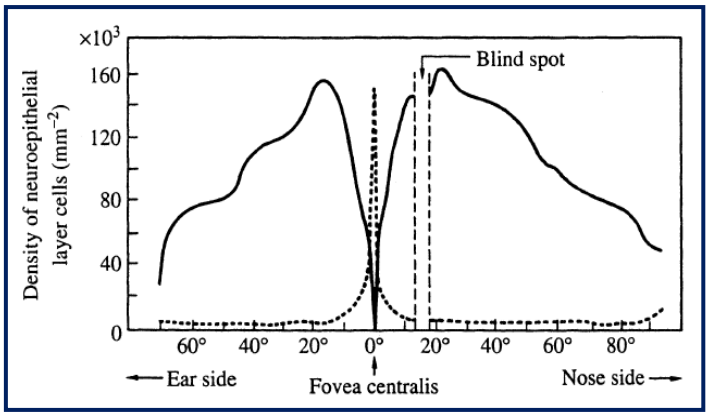

Fig. 2.1 Distribution of rods (solid line) and cones (broken line)

Human eyes can receive very wide range information of brightness, from about 100,000 lx, when seeing objects under direct sunlight, to about 0.0003 lx, when looking objects at night without moonlight. Although human visual system can adjust the pupil diameter to adapt different ambient brightness, but this still can't afford such large range variation of brightness. Thus, human eyes have a special mechanism for rods and cones to cooperate for fulfilling the requirement. When the ambient environment is quite dark, lower than 10^{-2} lx, only the rods will be active, and this called scotopic vision. However, when surrounding is brighter than 10 lx, the cones will take over the work and be active. This stage is then called the photopic vision. Besides, when the brightness of the environments is between 10^{-2}~10 lx, both cons and rods will be active in different ratio, and this is called mesopic vision [Fig. 2.2] [14].

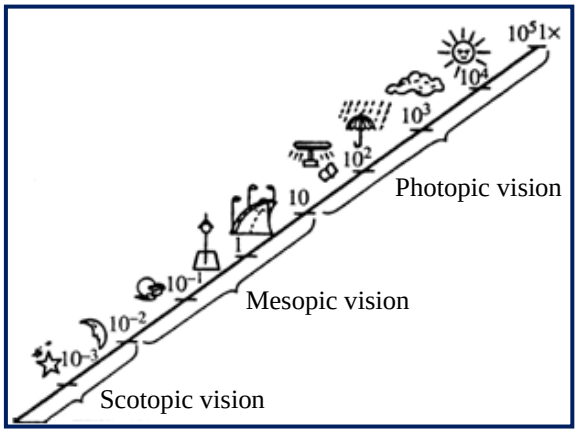

Fig. 2.2 Approximate brightness values for different visions

As a simple example, the ambient light source illuminates on a uniform diffuser with reflection efficiency ratio, ρ_{RS}, equals to 0.5, and then the light reflects into the eyes. First of all, the relationship between the luminance of the source, L_s, and the luminous exitance of the reflection surface, M_{RS}, can be describe by

$$M_{RS} = \rho_{RS} \pi L_S \quad \text{(Eq. 2.1)}$$

The π is the solid angle for a lambertian light, and is the luminance. After that, the incident light of the eye is modified by the pupil size, which assumes to be 15mm^2 at luminance of 1cd/m^2 and 44mm^2 at a luminance of 0.001cd/m^2. Thus, the luminous flux that illuminate on the retina can be calculated by

$$\phi_R = M_{RS} \times A_R \quad \text{(Eq. 2.2)}$$

Where ϕ_R is the luminous flux of the retinal, M_{RS} is the luminous exitance of the reflection surface, and A_R is the receiving area of the retinal.

Thus, the overall relationship between ambient brightness and human vision can be summed up in the following table [Table 2.1].

Table 2.1 Vision classification with ambient brightness

Illuminance (lx)	Luminance (cd/m^2)	Retinal Illuminance (td)	Classification		Spectral luminous efficiency
			Photo-receptor	Vision	
	10^5				
	10^4				
6×10^3	10^3		Cones	Photopic Vision	V(λ)
	10^2				
	10^1				
6×10^0	10^0	1.5×10^1			
	10^{-1}			Mesopic Vision	V*(λ)
	10^{-2}				
6×10^{-3}	10^{-3}	4.4×10^{-2}	Rods		
	10^{-4}			Scotopic Vision	V'(λ)
	10^{-5}				

2.1.2 Radiometry and photometry

The rod cells have different sensitivity through the visible spectrum, from 380nm to 780nm, in different ambient circumstances. In general, the spectral responsivity of a photoreceptor can be measured by the variation of its photocurrent. However, this method is hard to implement on the human visual system. Thus, the matching methods are introduced to get the wavelength sensitivity of rod cells. The most common methods include the direct comparison method, the step-by-step method, and the flicker method. Roughly speaking, all methods ask subjects to compare the brightness of the monochromatic light and the reference light, and then to modify the intensity of the monochromatic light till it is comparative to the reference one. The intensity of the monochromatic light will finally be recorded. Therefore, the wavelength responsivity of the rod cell is just the relative ratio of these intensities. The distribution of the average values derived from the direct comparison method, $\bar{V}_b(\lambda)$, is shown below [Fig. 2.3]. Besides, the difference between photopic vision and scotopic vision can be measured by modifying the brightness of reference light.

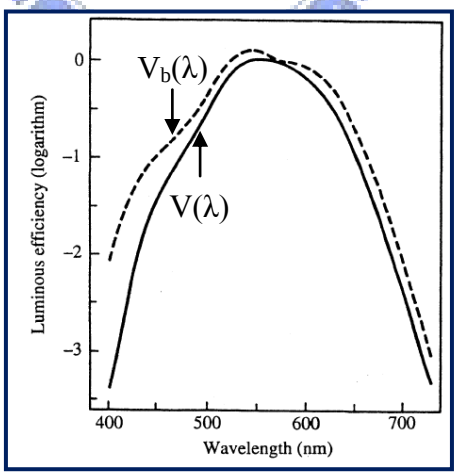

Fig. 2.3 Spectral luminous efficiency

The International Commission on Illuminance (CIE) then established two spectral responsivity curves as the worldwide standards. CIE also published the spectral luminous efficiency for photopic vision, $V(\lambda)$, which is based on the average observed values from seven studies involving 251 people with normal color vision, in

1924. In this standard, the rod has the highest sensitivity at the 555nm in photopic vision, and the highest sensitivity will translate to about 507nm in scotopic vision [Fig. 2.4]. The distribution variations between V(λ) and $V_b(\lambda)$ are significant, thus, the CIE has recommended $V_b(\lambda)$ separately in addition to V(λ), and still use V(λ) as the world standard.

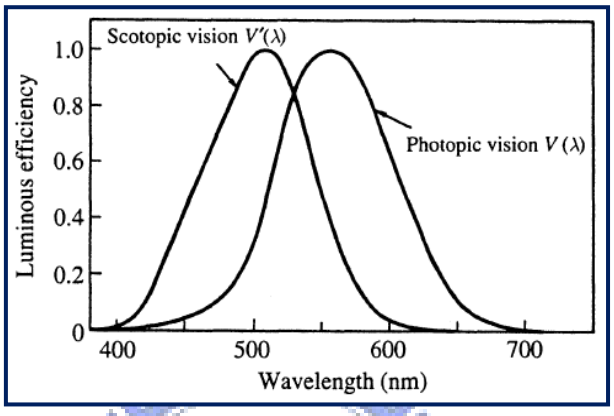

Fig. 2.4 Spectrum luminous efficiency in photopic and scotopic visions

Thus, the radiometric quantities can be converted into photometric quantities by the equation

$$(\text{Photometric quantity}) = K(\lambda) \times (\text{Radiometric quantity}) \qquad \text{(Eq. 2.3)}$$

Where K(λ) is the spectral luminous efficacies. One lumen is then defined as 1/683W of a monochromatic light with λ_m = 555nm. Therefore, the luminous efficacies of photopic and scotopic vision can be rewritten as

$$K(\lambda) = K_m V(\lambda) = 683V(\lambda) \qquad \text{(Eq. 2.4)}$$

$$K'(\lambda) = K'_m V'(\lambda) = 1700V'(\lambda) \qquad \text{(Eq. 2.5)}$$

Where K_m is the maximum luminous efficacy for the photopic vision, and K'_m is the maximum luminous efficacy for the scotopic vision. They are defined to be 683lm/W and 1700lm/W, respectively [Fig. 2.5].

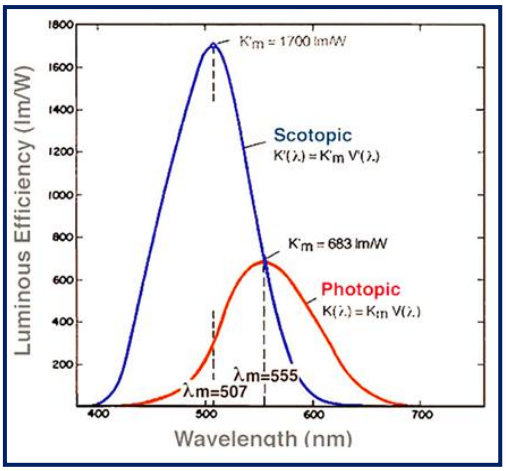

Fig. 2.5 Spectral luminous efficacy K(λ) and K'(λ)

The luminous flux of polychromatic light can be calculate by the following equation

$$\Phi_V = K_m \int \Phi_{e,\lambda}(\lambda) V(\lambda) d\lambda \qquad \text{(Eq. 2.6)}$$

Where Φ_v is the luminous flux that human perceived, the K_m is the maximum luminous efficacy, $\Phi_{e,\lambda}$ is the radiant flux that human eye received.

On the other hand, the spectral responsivities of the cones can also be measured by the same method, but the viewing angle of the observers should be narrowed lower than 2^o, this is due to the reason that cones are concentrated in the fovea centralis. After all, the spectral responsivities of the rod and cone cells can be measured, and this can help us to comprehend the mechanism of the visual system much more.

2.1.3 Color vision theory

Human are curious for a long time about the color vision mechanism. Many hypotheses had been proposed. The two most convincing hypotheses are the trichromatic theory, proposed by Thomas Young and Hermann von Helmholtz, and the opponent-color theory, proposed by Ewald Hering.

The trichromatic theory was first proposed by Young in 1802, and extended by Helmholtz in 1894. The theory postulates that the retina comprises three types of photoreceptor (cones), which sense red, green, and blue colors respectively. Thus, all colors are characterized by the degree of response of three photoreceptors [Fig. 2.6].

In fact, the peaks in the model do not actually correspond to red, green, and blue, so it is more accurate to describe them as long-, medium-, and short- wavelength photoreceptors. The theory is based on the experimental result that almost all colors can be reproduced by properly mixing three lights, usually red, green, and blue. Besides, trichromatic theory has been used in many fields, such as color TV sets, photography, color printing, etc., and has been proved to have very great color reproduction ability. Accordingly, trichromatic theory is not only a simple but also a realistic and convincing hypothesis.

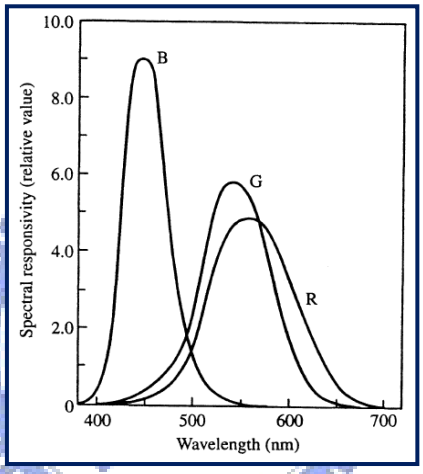

Fig. 2.6 Spectral responsivities of red (R), green (G), and blue (B) photoreceptors in the trichromatic theory

On the other hand, the opponent-color theory was proposed by Hering in 1878, which also postulates that the retina comprises three types of photoreceptors, but in different with the trichromatic theory, they responds to red-green, yellow-blue, white-black opponencies respectively. The colors are also characterized by the degree of response of these photoreceptors. However, the response signals are a little different than the former theory. For example, the first type of photoreceptor responds in a positive fashion to red, and in a negative fashion to green [Fig. 2.7]. The theory is based on empirical fact showing that there can be a yellowish red and a bluish red but no greenish red. Thus, the green and red are opponent color.

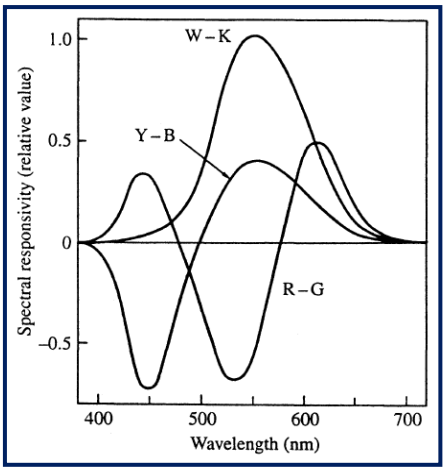

Fig. 2.7 Spectral responsivities of red-green (R-G), yellow-blue (Y-B), and white-black (W-K) photoreceptors in the opponent-color theory

Both theories are based on experimental results and can explain various color vision phenomena without facing any contradictions. Besides, in 1964, Brown and Wald used microscopic techniques to confirm the presence of three types of cone with peak wavelength 450, 525, 555nm respectively [Fig. 2.8].

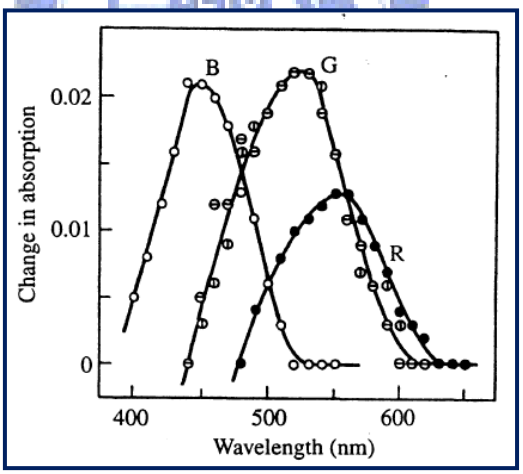

Fig. 2.8 Spectral absorption in human cones

This gives the direct evidence of the trichromatic theory. Furthermore, attribute to the improvement in electrophysiology, in 1953, Svaetichin had found an opponent-type spectrum response by inserting microelectrodes into the retina, which is known as the S potential 1953. The S potential was first thought to support the opponent-color theory.

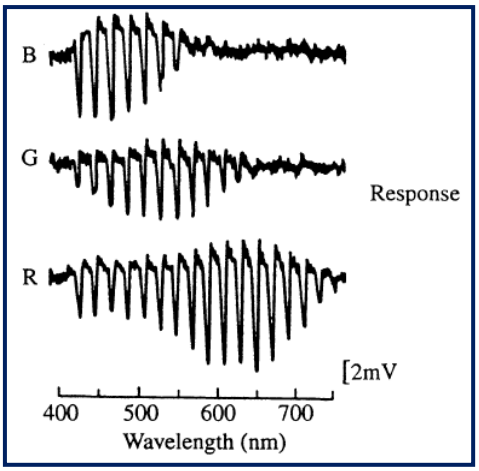

Fig. 2.9 S potential in the crap retina

Tomita also did the same experiment on carp in 1967 [Fig. 2.9]. By his much detailed measurements, it shown that the signals actually came from a region that is several tens of um distance from the cones. Thus, from the experimental results given above, human eyes can be regarded as three photoreceptors with peak responses at 450,525, 555nm, and the received response signals will be translate into opponent-color information before they are transmitted to the brain.

Based on the knowledge of human visual response, a lot of models were developed to explain the phenomena of color vision. The most convincing one is the stage theory, which is based on the results of psychological experimentations, of microscopic spectral measurements, and of electrophysiological measurements. In this model, the brightness response of the rods and the red, green, blue response of the cones are received at first stage. After that, the rods response is directly related to the brightness in scotopic vision. Besides, the cones responses are divided into three signals, two opponent-color responses (R-G, Y-B) and the brightness response in photopic vision [Fig. 2.10].

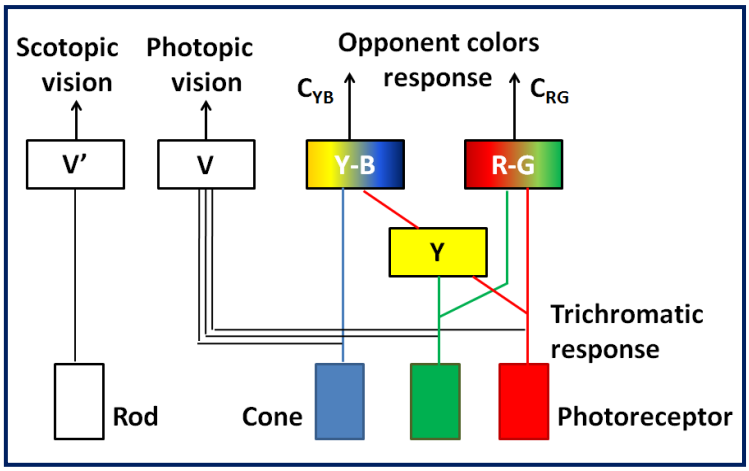

Fig. 2.10 Color vision model based on stage theory

Thus, the human visual system is assumed to have a trichromatic response at the cone level and an opponent-colors response in later stage.

2.2 Fundamental Color Science

2.2.1 CIE color system

Based on the human visual model constructed before, two color models were proposed to quantify the color information. They are color appearance system and color mixing system. Color appearance system is based on color perception, but are defined in terms of material standards (ex: color chips) and their appearance under specific illumination conditions. On the other hand, color mixing system is based on the amounts of mixed colored light necessary to obtain a color match to a test color in a color mixing experiment. Generally speaking, the color appearance systems are usually used in the dye industry and house decorations, and the color mixing systems are common applied in lighting and display fields. Thus, we will only introduce the color mixing system here.

The most famous color mixing system was developed by the CIE. CIE established the standard color matching functions in 1931 based on the following principles (CIE 1986, 2004a).

1. The reference stimuli [R], [G], [B] are monochromatic lights of wavelength λ_R=700.0nm, λ_G=546.1nm, λ_B=435.8nm, respectively.

2. The basic stimulus is the white color stimulus of the equienergy spectrum. The amounts of the reference stimuli, [R], [G], and [B], are required to match the basic stimulus are in the ratio 1.0000:4.5907:0.0601 when expressed in photometric units, and 72.0966:1.3791:1 when expressed in radiometric units.

Color matching functions are the amounts of the reference stimuli needed to match monochromatic stimuli of each wavelength. Due to the requirements set above, CIE adopted an average data from Guild and Wright's experimental results as the color matching functions [Fig. 2.11].

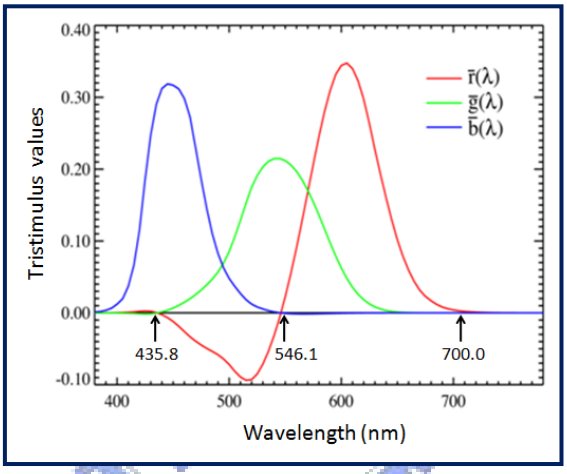

Fig. 2.11 Color matching functions of the CIE 1931 RGB color system

Thus, by additive color mixing methods, every monochromatic light can be describe as

$$[F_\lambda] = R[R] + G[G] + B[B] \qquad \text{(Eq. 2.7)}$$

Where $[F_\lambda]$ is an arbitrary monochromatic light, [R], [G], and [B] are reference stimuli, and R, G, and B, tristimulus values, are the weighting of each stimulus respectively. This system is then called the CIE 1931 RGB Color Specification System, and the RGB color space is received by projecting these three weighting vectors onto a unit plane by the following equations [Fig. 2.12].

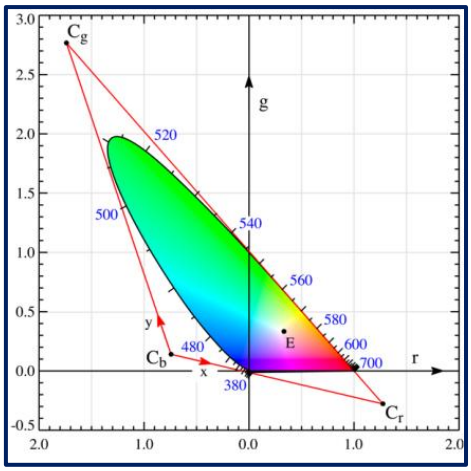

Fig. 2.12 Chromaticity diagram for the CIE 1931 RGB color system

$$r = \frac{R}{R+G+B} \quad \text{(Eq. 2.8)}$$

$$g = \frac{G}{R+G+B} \quad \text{(Eq. 2.9)}$$

$$b = \frac{B}{R+G+B} \quad \text{(Eq. 2.10)}$$

However, in this system, the R value is negative from 435.8nm to 546.1nm, that is due to the experimental results that the [G] and [B] stimulus can't mix the same as the test light until using [R] stimulus to decrease the chromaticity of the test light, and this may cause some problems in the following calculations. Thus, CIE introduced a transformation matrix to receive another color matching functions, [X], [Y], and [Z], or $\tilde{x}(\lambda)$, $\tilde{y}(\lambda)$, and $\tilde{z}(\lambda)$ [Fig. 2.13]. The new tristimulus values, X, Y, and Z can be received by the following matrix. .

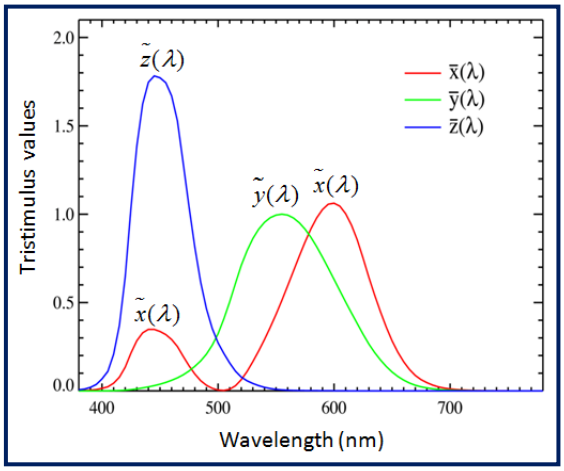

Fig. 2.13 Color matching functions of the CIE 1931 XYZ color system

$$\begin{pmatrix} X \\ Y \\ Z \end{pmatrix} = \begin{pmatrix} 2.7689 & 1.7517 & 1.1302 \\ 1.0000 & 4.5907 & 0.0601 \\ 0.0000 & 0.0565 & 5.5943 \end{pmatrix} \begin{pmatrix} R \\ G \\ B \end{pmatrix} \quad \text{(Eq. 2.11)}$$

This is called the CIE 1931 Standard Colorimetric System. One special characteristic of this system is that the matching function [Y] is identical to the spectral luminous efficiency function V(λ). Therefore, the tristimulus value Y can directly express the photometric quantity. As the same, the XYZ color space can also be received by projecting three weighting vectors onto a unit plane [Fig. 2.14].

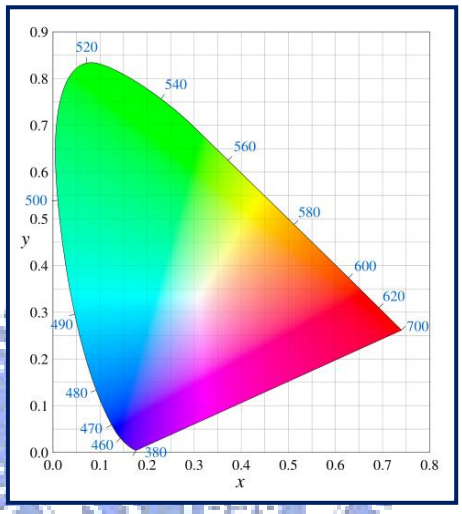

Fig. 2.14 Chromaticity diagram for the CIE 1931 XYZ color system

After all, the color of any light spectrum can be described by the tristimulus values of the system, and find a position on the chromaticity diagram by the following equations. The constant κ is selected such that the tristimulus value Y can yield a value 100 for the perfect reflecting object (R(λ)=1 for all λ in the visible range).

$$X = \kappa \int_{vis} \Phi(\lambda)\tilde{x}(\lambda)\, d\lambda \quad \text{(Eq. 2.12)}$$

$$Y = \kappa \int_{vis} \Phi(\lambda)\tilde{y}(\lambda)\, d\lambda$$

$$Z = \kappa \int_{vis} \Phi(\lambda)\tilde{z}(\lambda)\, d\lambda$$

$$\kappa = \frac{100}{\int_{vis} \Phi(\lambda)\tilde{y}(\lambda) d\lambda}$$

$$x = \frac{X}{X+Y+Z} \qquad \text{(Eq. 2.13)}$$

$$y = \frac{Y}{X+Y+Z}$$

$$z = \frac{Z}{X+Y+Z}$$

Although CIE 1931 XYZ color system is a good system and used widely in various fields, it also has incomplete in some aspects, especially in color space uniformity. A uniform color space is expected to have equal distance on the chromaticity diagram with human perception. Thus, CIE published a series of new color systems to improve the color uniformity, such as CIE 1964 W*U*V*, CIE 1976 LAB, and CIE 1976 LUV. The new color systems are derived by some linear or nonlinear transformations of the tristimulus values. The last two systems are also well-known and applied in many fields.

2.2.2 Correlated color temperature

As mentioned before, a color stimulus can be specified in three dimensions by the tristimulus values and in two dimensions by the chromaticity coordinates. However, when describing the color stimulus of a white light, it can also be specified by one parameter, the correlated color temperature (CCT).

Color temperature, T_c, indicates that the chromaticity of the given radiation corresponds to the chromaticity of the radiation from a black body of absolute temperature T_c. On the other hand, correlated color temperature, T_{cp}, is defined as the temperature of the black body whose chromaticity is nearest to the given radiation. The color distance is generally calculated on the CIE 1960 UCS color space. Thus, the isotemperature lines are received by connecting the points with the same correlated color temperature [Fig. 2.15].

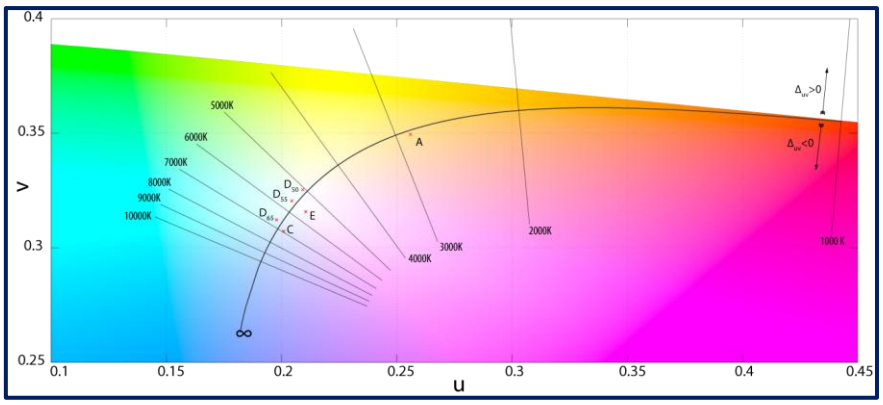

Fig. 2.15 Planck locus and iso-temperature lines

Black body locus is received by calculating the chromaticity of the black body radiation with different temperature. The black body radiation spectrum is described by Max Planck in 1901.

$$M_{e,\lambda}(\lambda) = c_1 \lambda^{-5} \left\{ \exp\left(\frac{c_2}{\lambda T}\right) - 1 \right\}^{-1} \quad \text{(Eq. 2.13)}$$

$$c_1 = 2\pi hc^2$$

$$c_2 = \frac{hc}{\kappa}$$

Where h is the Planck's constant and κ is Boltzmann's constant with values 6.626×10^{-34} (Js) and 1.38×10^{-23} (JK^{-1}) respectively. Besides, c is the speed of light in vacuum, 3×10^{8}(m/s), T is the temperature of black body with the unit in 'degree Kelvin', and λ is the wavelength of the radiation.

2.2.3 Color Rendering Index

Color rendering is used to describe the slight color shift of the object color when using different illuminants. Thus, the higher color rendering properties of an illuminant stands for the better color appearance performance. There are lots of methods used to evaluate this property by means of comparing the difference in spectral distribution or in color appearance of a series of object colors. The most well known and used one is proposed by the CIE in 1995, called the color rendering index. This index expresses numerically the degree of matching of color appearance of the specific color chips under a test light source and a reference illuminant.

The reference illuminant in CIE calculation is defined by two methods, depending on the color temperature of the test light source. When the test light source has color temperature lower than 5000K, the black body radiator is used as the reference illuminant. On the other hand, when the test light source is higher than 5000K, a CIE daylight illuminant is used as the reference illuminant. The CIE daylight illuminant comes from the daylight measurement data that collected and analyzed by CIE in the early 1960s. Due to the measurement result, the daylight spectral distribution, $S_D(\lambda)$, can be received by the combination of three eigenvectors, $S_0(\lambda)$, $S_1(\lambda)$, and $S_2(\lambda)$ [Fig. 2.16] [14].

$$S_D(\lambda) = S_0(\lambda) + M_1 S_1(\lambda) + M_2 S_2(\lambda) \qquad \text{(Eq. 2.13)}$$

$$M_1 = \frac{(-1.3515 - 1.7703x_D + 5.9114y_D)}{(0.0241 + 0.2562x_D - 0.7341y_D)}$$

$$M_2 = \frac{(0.03 - 31.442x_D + 30.0717y_D)}{(0.0241 + 0.2562x_D - 0.7341y_D)}$$

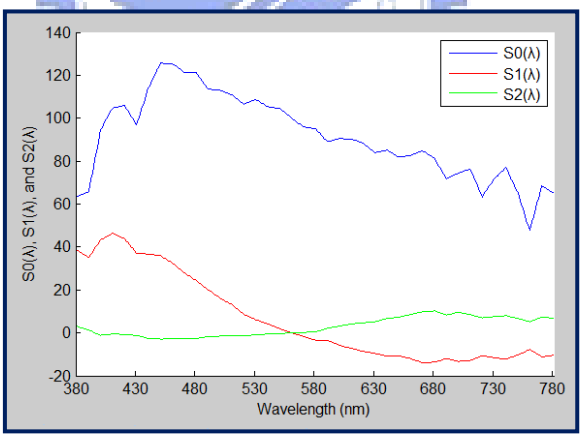

Fig. 2.16 Three eigenvectors for constituting daylight

Where x_D and y_D are the color coordinates from the daylight locus, which are relative to the chosen color temperature.

When $4000K \leqq T_{cp} \leqq 7000K$

$$x_D = \frac{-4.0607 \times 10^9}{T_{cp}^3} + \frac{2.9678 \times 10^6}{T_{cp}^2} + \frac{0.09911 \times 10^3}{T_{cp}} + 0.244063 \qquad \text{(Eq. 2.14)}$$

When $7000K \leqq T_{cp} \leqq 25000K$

$$x_D = \frac{-2.0064 \times 10^9}{T_{cp}^3} + \frac{1.9081 \times 10^6}{T_{cp}^2} + \frac{0.24748 \times 10^3}{T_{cp}} + 0.23704 \qquad \text{(Eq. 2.15)}$$

With

$$y_D = -3x_D^2 + 2.87x_D - 0.275 \quad \text{(Eq. 2.16)}$$

After defined the reference illuminant, CIE selected fifteen specific color chips as the test colors, and the color rendering index are calculated by the color difference of these chips under the test light source and the reference illuminant. The Munsell color chips and the spectral reflectance are shown as below [Fig. 2.17(a), 2.17(b), 2.18] [15].

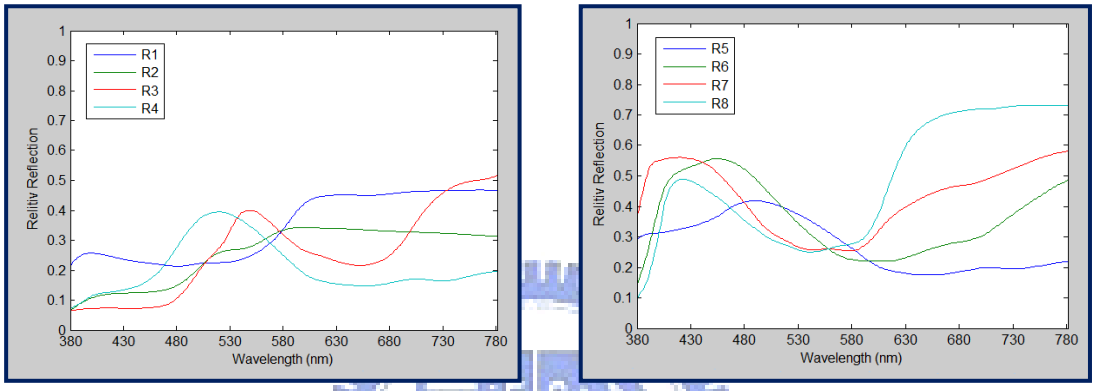

(a) Color chip no. 1~4 **(b)** Color chip no. 5~8

Fig. 2.17 Reflection spectra of standard CRI calculation color chips

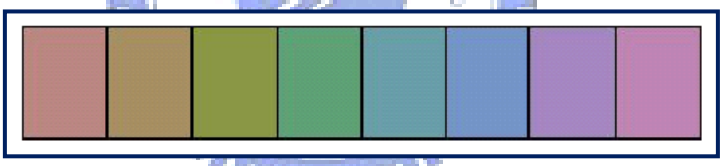

Fig. 2.18 Standard Munsell color chips of the CRI calculation

Generally speaking, test colors, which in Munsell notation have V/C value, Munsell value/Munsell chroma, in the range from 6/4 to 6/8, are colors with medium lightness and medium saturation. They are used to represent the average object colors. The average number of this eight color rendering indices is known as the CIE General Color Rendering Index, R_a.

For the computation of color difference, CIE 1964 W*U*V* color space was selected due to its great color uniformity [15]. The transformation of the color coordinates from CIE 1931 XYZ to CIE 1964 W*U*V* can be done by the following formulae

$$W^* = 25Y^{\frac{1}{3}} - 17 \qquad \text{(Eq. 2.17)}$$

$$U^* = 13W^*(u - u_n)$$

$$V^* = 13W^*(v - v_n)$$

The u and v in equation 2.17 come from the CIE 1960 UCS chromaticity diagram. The converting formulae are given by

$$u = \frac{4X}{(X+15Y+3Z)} = \frac{4x}{(-2x+12y+3)} \qquad \text{(Eq. 2.18)}$$

$$v = \frac{6Y}{(X+15Y+3Z)} = \frac{6y}{(-2x+12y+3)}$$

Most applications do not use the CIE 1964 W*U*V* nowadays, and replacing it by the CIE 1976 L*a*b* or the CIE 1976 L*u*v* color spaces is also theoretically available. However, there are only minor changes between the different systems. Thus, CIE still adopted CIE 1964 W*U*V* for the color rendering computation [14].

In most cases, the chromaticity coordinates of the test source and the reference illuminant are not matching, and the chromatic adaptation is used for compensating this small deviation. The most fundamental chromatic adaptation model is proposed by Johannes von Kries in 1902. In this hypothesis, he assumed that human eye have three types of receptors, each for red, green, and blue respectively, and these three receptors will modify their sensitivity due to the environment lighting. For example, when a human walks from outside, with general daylight, into a house with incandescent lamp illumination, the sensitivity of red receptor will decrease. This is due to the reason that the incandescent lamp has larger portion of long-wavelength spectrum than the daylight does [Fig. 2.19]. Thus, the tristimulus values will also be changed. The transformation of this phenomenon can be written as the following matrix.

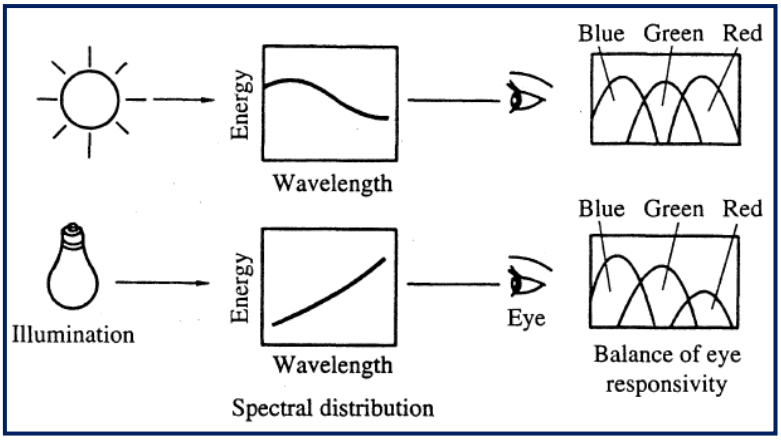

Fig. 2.19 Illumination adaptation of visual receptors

$$\begin{pmatrix} X' \\ Y' \\ Z' \end{pmatrix} = \begin{pmatrix} a_{11} & a_{12} & a_{13} \\ a_{21} & a_{22} & a_{23} \\ a_{31} & a_{32} & a_{33} \end{pmatrix} \begin{pmatrix} X \\ Y \\ Z \end{pmatrix} \quad \text{(Eq. 2.19)}$$

Where the X′, Y′, and Z′ are the tristimulus values after chromatic adaptation, and the X, Y, and Z are the original tristimulus values. Beside, elements a_{ij} of the matrix is obtained from the tristimulus values of the test light and the reference light. The basic idea of von Kries model is that the object color seen by human eye is the combination of its original color and the light source information. Thus, the chromatic adaptation simply withdraws the light source information from the observed object color, and then combines the other light source information into it to represent the object color appearance under different observing surrounding. The most general term in color appearance model is come from this idea and are written as

$$\frac{R}{R_0} = \frac{R'}{R'_0} \quad \text{(Eq. 2.20)}$$

$$\frac{G}{G_0} = \frac{G'}{G'_0}$$

$$\frac{B}{B_0} = \frac{B'}{B'_0}$$

The R, G, and B are object tristimulus values observed under test illuminant, and the R′, G′, and B′ are the object tristimulus values observed under reference illuminant. Besides, R_0, G_0, and B_0 are tristimulus values of test illuminant, and R'_0, G'_0, and B'_0 are tristimulus values of reference illuminant.

Therefore, CIE developed from von Kries' hypothesis and established the following modification equations for calculating the object color difference when the object is illuminated under different light sources.

$$u_k^{'} = u_r \qquad \text{(Eq. 2.21)}$$
$$v_k^{'} = v_r$$

$$u_{k,i}^{'} = \frac{\left(10.872+0.404c_r\frac{c_{k,i}}{c_k}-4d_r\frac{d_{k,i}}{d_k}\right)}{\left(16.518+1.481c_r\frac{c_{k,i}}{c_k}-d_r\frac{d_{k,i}}{d_k}\right)}$$

$$v_{k,i}^{'} = \frac{5.52}{\left(16.518+1.481c_r\frac{c_{k,i}}{c_k}-d_r\frac{d_{k,i}}{d_k}\right)}$$

With coefficients c and d

$$c = \frac{(4-u-10v)}{v}$$

$$d = \frac{(1.708v+0.404-1.481u)}{v}$$

In the equation 2.21, the u'_k and v'_k are the chromaticity coordinates of the test source after applying the chromatic adaptation correction, and the u_r and v_r are the chromatic coordinates of the reference illuminant. Besides, the $u'_{k,i}$ and $v'_{k,i}$ are the chromaticity coordinates of the test colors after applying the chromatic adaptation correction. The c_r and d_r are coefficients that computed from the chromaticity coordinates u_r and v_r. As the same, the $c_{k,i}$ and $d_{k,I}$ are coefficients that computed from the chromaticity coordinates $u_{k,i}$ and $v_{k,i}$.

Thus, using the spectral distribution can calculate the tristimulus values at first, and then convert the tristimulus values into CIE 1964 W*U*V* color space with chromaticity adaptation. After all, the rendering index can be obtained by the color difference ΔE_i.

$$\Delta E_i = \langle \left(U^*_{r,i} - U^*_{k,i}\right)^2 + \left(V^*_{r,i} - V^*_{k,i}\right)^2 + \left(W^*_{r,i} - W^*_{k,i}\right)^2 \rangle^{\frac{1}{2}} \qquad \text{(Eq. 2.22)}$$

$$R_i = 100 - 4.6\Delta E_i \qquad \text{(Eq. 2.23)}$$

$$R_a = \frac{(\sum_{i=1}^{8} R_i)}{8} \qquad \text{(Eq. 2.23)}$$

Generally speaking, the light sources should have R_a value higher than 80 for general applications, and much higher in specific applications, such as jewelry stores, galleries [16].

Chapter 3

Simulations

The objective of the thesis is to establish a software platform that can simulate the objective color performance, CCT and CRI, subjective to the combination of various light sources, which is first attributed by a LED-based system. Thus, in this chapter, the frameworks of the software platform will be described at first. After that, the simulation setups will be given, and finally is a simple demo of the overall GUI program.

3.1 Introduction of the Simulation

In this section, we aim to construct a MATLAB® based graphic user interface (GUI) platform to calculate the lighting performance (CCT, CRI) under different lighting options. This function is not available when using traditional light sources, which have fixed spectrum power distributions (SPDs), and their CRI values and CCT values are unchangeable. However, due to the emergence of LEDs, which have near monochromatic SPDs, light sources gain the flexibility of changing SPDs but maintain the same CCT value. Therefore, many CRI values are corresponding to a given CCT. However, the calculations of the problem are very sophisticated and are not obvious to solve directly. Thus, developing a tool to solve the problem is an important issue for LEDs' future applications.

The basic idea of our simulation tool is that the user can import the measured SPDs, and the tool can calculate the maximum CRI value under the requirements that the user sets. The available requirements in our tool are CCT value and the mixing light source numbers. Besides, in order to give the tool more flexibility, it is defaulted to have ten import lighting source channels.

The flowchart of the simulation tool is shown below [Fig. 3.1]. The first step will ask the user to import the spectrum data, expected CCT, and the number of mixing light sources. After that, the program will base on the given requirements to calculate all possible mixing ratios that can fulfill the CCT coordinates in the second stage. Therefore, in the third stage, the program only needs to calculate the CRI values of the candidate ratios and then selects the highest one. After the highest CRI value is received, the program will show the CRI value, the weightings of the light sources and plot a figure of the mixing SPD.

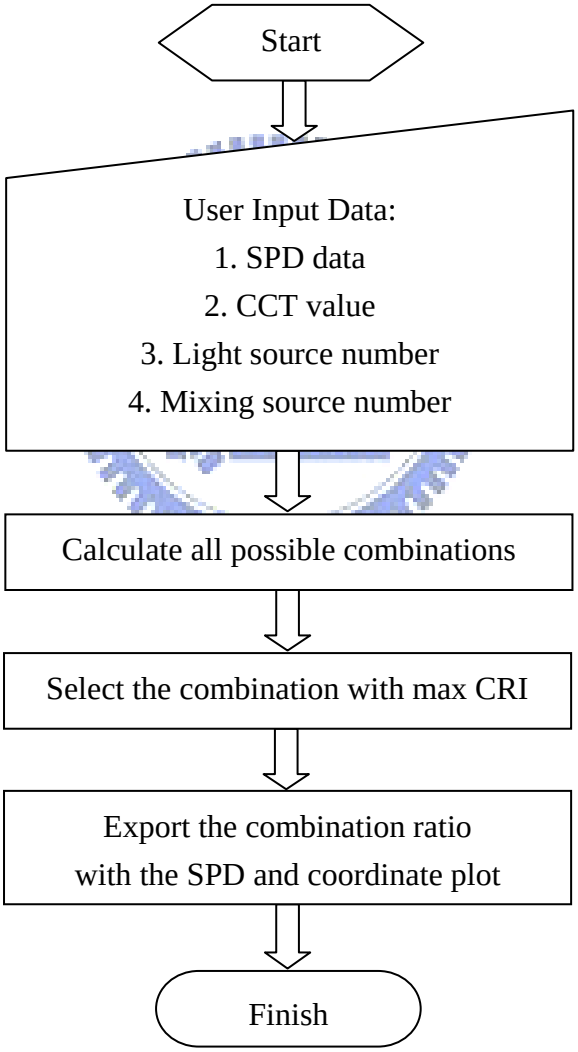

Fig. 3.1 Flowchart of the simulation

3.2 Simulation Setups

3.2.1 Simulation of basic parameters

The SPD of LEDs is the most basic information in the simulation. Thus, the ability to simulate the LED SPD is important for the preset simulations. The SPD of the phosphor white LED is much more complicated and case by case. Thus, we only simulate the primary color LED SPD here. Generally, the primary color LED SPD has a Gaussian shape distribution with different full-width-half-maximum (FWHM). Many equations are used to simulate the profile, and they are usually expressed as an equation with two variables, the primary wavelength and the FWHM value. The most common model is shown as bellow and comes from Yoshi Ohno [17].

$$S_{LED}(\lambda, \lambda_0, \Delta\lambda_{0.5}) = \frac{\{g(\lambda,\lambda_0,\Delta\lambda_{0.5}) + 2\times g^5(\lambda,\lambda_0,\Delta\lambda_{0.5})\}}{3} \quad \text{(Eq. 3.1)}$$

$$g(\lambda, \lambda_0, \Delta\lambda_{0.5}) = \exp\left[-\left\{\frac{(\lambda-\lambda_0)}{\Delta\lambda_{0.5}}\right\}^2\right]$$

Here we use the same equation as our LED model, and simulate the LED SPD of a AVaGO® high power RGB light source, ADJD-MJ50, from the data sheet. The measurement and simulation SPD are shown below [Fig. 3.2]. The correlation coefficient is larger than 98%. Thus, the variations between the two normalized SPDs are very small. Thus, this LED SPD model is used for our previous design simulation.

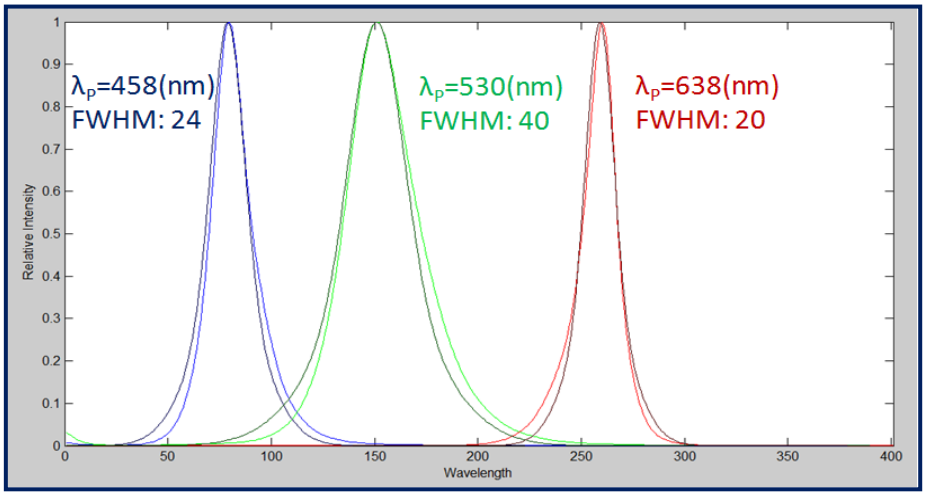

Fig. 3.2 Simulation LED SPDs and Measurement LED SPDs
(Darker lines for the simulation SPDs and lighter lines for the measurement SPDs)

In our simulation flow, the program will calculate all possible mixing ratios that have the same CCT value. Thus, by the black body radiation equations given before, the SPDs of different temperature can be calculated, and then received the chromatic coordinates. Therefore, the black body locus can be drawn with the expected CCT lines [Fig. 3.3].

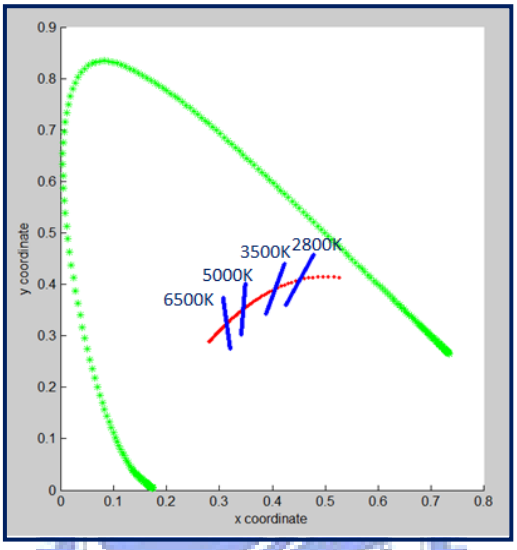

Fig. 3.3 Black body locus with CCT lines

Choosing the correct reference illuminant is important for the calculation of CRI values. As mentioned before, CIE selected different reference illuminants for the different CCT value light sources. The CIE daylight illuminant is used when the CCT value is higher than 5000K, and the black body radiation is used when the CCT value is lower than 5000K. In order to simplify the application, CIE established the SPDs of the standard illuminant at general CCT values, such as D65, D55, D50, and A. The diagrams of the calculated CIE daylight SPDs and the standard illuminants are shown below [Fig. 3.4], and it is obvious that the simulated SPDs are corresponding to the standard ones.

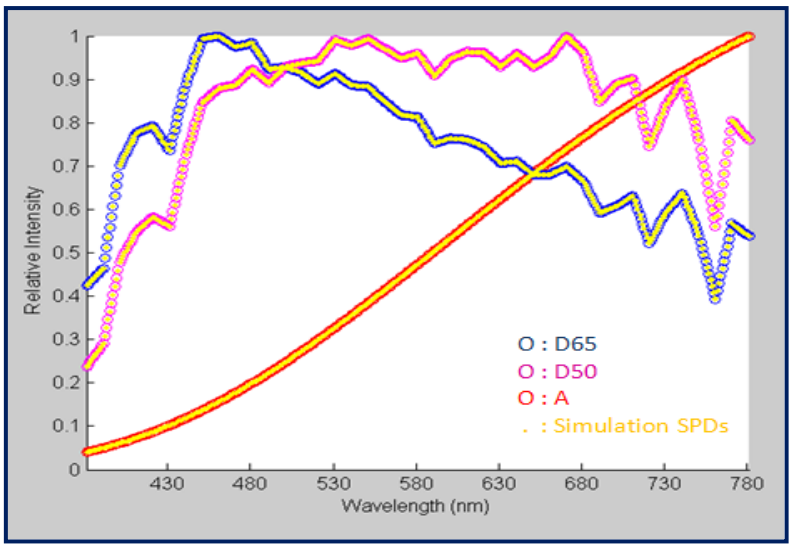

Fig. 3.4 CIE daylight SPDs and standard illuminant SPDs

3.2.2 Modification of the mixing ratio

After showing the ability of simulating some fundamental parameters, the method of modifying the mixing ratio will be mentioned here. In our research, we first proposed a modify method based on the simplification of the relationships between SPD and chromaticity coordinates. In this method, we first consider an arbitrary SPD, and then we try to modify the SPD at two wavelengths, λ_1 and λ_2, with different signs, one positive and one negative, and the same weighting [Fig. 3.5].

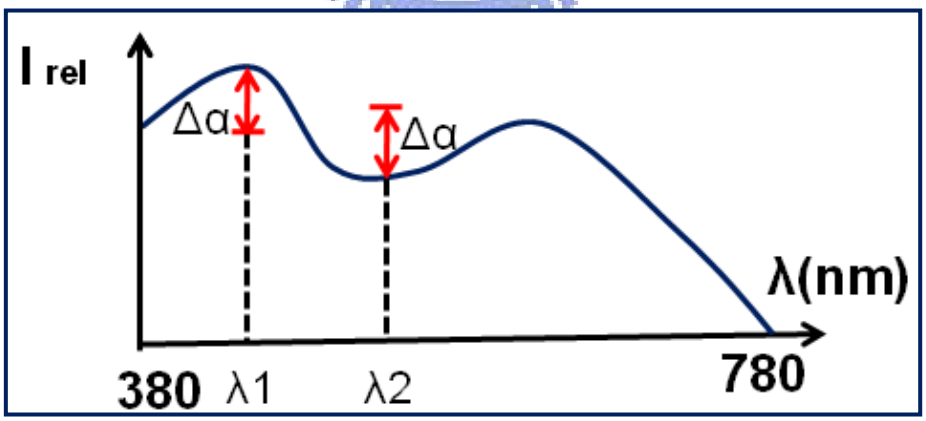

Fig. 3.5 Modification concept in the beginning method

After that, the chromaticity coordinates of the original SPD and the SPD after modification, SPD', can be calculated by the following equations (Eq. 3.2 ~ Eq. 3.4). Thus, the movement of the chromaticity coordinates can be described as the functions of modify wavelength (Eq. 3.5).

$$X = \int_{380}^{780} SPD \times \tilde{x}(\lambda) \qquad \text{(Eq. 3.2)}$$

$$Y = \int_{380}^{780} SPD \times \tilde{y}(\lambda)$$

$$Z = \int_{380}^{780} SPD \times \tilde{z}(\lambda)$$

$$X' = \int_{380}^{780} SPD' \times \tilde{x}(\lambda) \qquad \text{(Eq. 3.3)}$$

$$Y' = \int_{380}^{780} SPD' \times \tilde{y}(\lambda)$$

$$Z' = \int_{380}^{780} SPD' \times \tilde{z}(\lambda)$$

$$x = \frac{X}{X+Y+Z} \qquad \text{(Eq. 3.4)}$$

$$y = \frac{Y}{X+Y+Z}$$

$$z = \frac{Z}{X+Y+Z}$$

$$\Delta x = \frac{\Delta\alpha[\Delta\tilde{x}(\lambda_1,\lambda_2) - x(\Delta\tilde{x}(\lambda_1,\lambda_2)+\Delta\tilde{y}(\lambda_1,\lambda_2)+\Delta\tilde{z}(\lambda_1,\lambda_2))]}{[X+Y+Z+\Delta\alpha(\Delta\tilde{x}(\lambda_1,\lambda_2)+\Delta\tilde{y}(\lambda_1,\lambda_2)+\Delta\tilde{z}(\lambda_1,\lambda_2))]} \qquad \text{(Eq. 3.5)}$$

$$\Delta y = \frac{\Delta\alpha[\Delta\tilde{y}(\lambda_1,\lambda_2) - y(\Delta\tilde{x}(\lambda_1,\lambda_2)+\Delta\tilde{y}(\lambda_1,\lambda_2)+\Delta\tilde{z}(\lambda_1,\lambda_2))]}{[X+Y+Z+\Delta\alpha(\Delta\tilde{x}(\lambda_1,\lambda_2)+\Delta\tilde{y}(\lambda_1,\lambda_2)+\Delta\tilde{z}(\lambda_1,\lambda_2))]}$$

$$\Delta z = \frac{\Delta\alpha[\Delta\tilde{z}(\lambda_1,\lambda_2) - z(\Delta\tilde{x}(\lambda_1,\lambda_2)+\Delta\tilde{y}(\lambda_1,\lambda_2)+\Delta\tilde{z}(\lambda_1,\lambda_2))]}{[X+Y+Z+\Delta\alpha(\Delta\tilde{x}(\lambda_1,\lambda_2)+\Delta\tilde{y}(\lambda_1,\lambda_2)+\Delta\tilde{z}(\lambda_1,\lambda_2))]}$$

The equations show that the movement of chromaticity coordinates is depending on the difference of three matching functions at wavelength λ_1 and λ_2. Due to the reason that the denominators of the equation 3.5 are always positive and the term $\Delta\alpha$ can also be defined to be positive, the numerators of equation 3.5 can be regarded as the indicators of the coordinate movement. Therefore, we expected to use the parameter, M_{dir}, as the guideline for the program to modify the mixing ratio (Eq. 3.6).

$$x_{dir} = \Delta\tilde{x}(\lambda_1, \lambda_2) - (\frac{x}{1-x})(\Delta\tilde{y}(\lambda_1, \lambda_2) + \Delta\tilde{z}(\lambda_1, \lambda_2)) \quad \text{(Eq. 3.6)}$$

$$y_{dir} = \Delta\tilde{y}(\lambda_1, \lambda_2) - (\frac{y}{1-y})(\Delta\tilde{x}(\lambda_1, \lambda_2) + \Delta\tilde{z}(\lambda_1, \lambda_2))$$

$$z_{dir} = \Delta\tilde{z}(\lambda_1, \lambda_2) - (\frac{z}{1-z})(\Delta\tilde{x}(\lambda_1, \lambda_2) + \Delta\tilde{y}(\lambda_1, \lambda_2))$$

$$M_{dir} = (a \times x_{dir}) + (b \times y_{dir}) + (c \times z_{dir})$$

Where a, b, and c are the sign factor for the indicator, and the values are depending on the relative position of current coordinates and the target coordinates.

However, after some previous tests of this parameter, M_{dir}, we found out that the parameter is only correct for mono-wavelength modulation. This is due to the reason that the assumption we set in the beginning only considers to modify two mono-wavelengths. Therefore, the profile of the light source should be taken into consideration in practical computation. Thus, this indicator will be too tedious to use.

After all, we gave up using M_{dir} as the indicator for modifying the light source mixing ratio, and turned back to take the color difference on the chromaticity diagram as the parameter for movement judgment. The color difference we take is the ΔE_{xy} on CIE 1931 xyz chromaticity diagram. Although the other color system has better uniformity, the calculation simplicity is the prior issue that we consider here.

Here we use an example to explain the modification process of the program. If we have four LED with mixing chromaticity points at (0.38, 0.28) and the target point at (0.30, 0.31) as shown in Fig. 3.6(a). Thus, the program will first calculate the eight possible modification chromaticity points, each is received by increasing or decreasing one of the four LED lightness level [Fig. 3.6(b)]. After that, the program will modify the LED which can reduce the color difference to a minimum value. Therefore, the program can approach the target coordinates by repeating the modification. The program will finally stop when the color difference is less than 0.005, which is set by the half distance of the neighboring discrete CCT coordinates

we setup before, and it is believed that the human eye cannot distinguish the color difference at this scale [14]

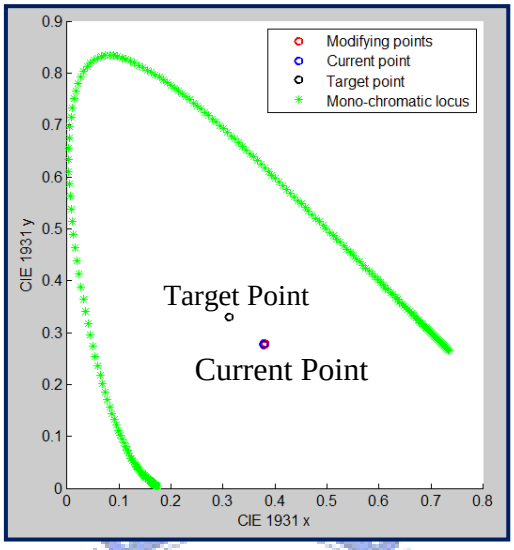

Fig. 3.6(a) Relative position of the current coordinates and the target coordinates

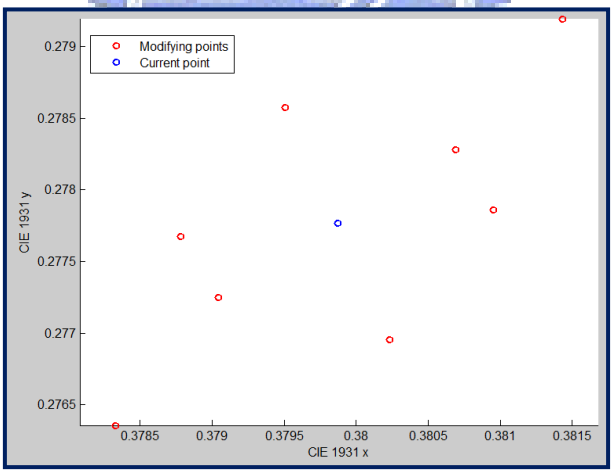

Fig. 3.6(b) Chromaticity coordinates after modifying the mixing ratio

3.3 Simulation Results

After simulating the basic elements of the calculation, we used the MATLAB® to create the GUI panel of the program [Fig. 3.7].

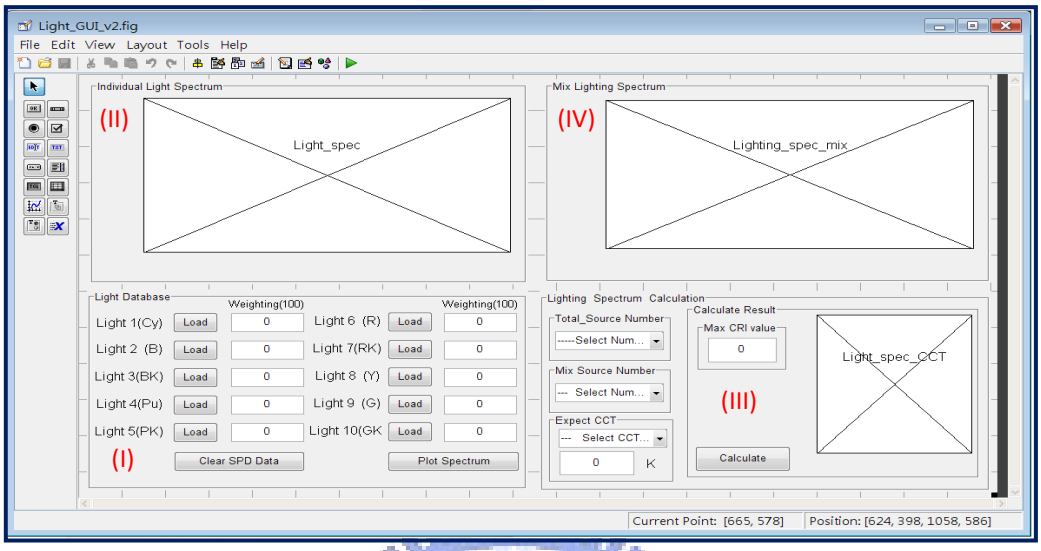

Fig. 3.7 GUI panel

The GUI panel is divided into four parts, region I, region II, region III, and region IV, as also be shown in the previous figure. The region I is used for the user to import the measurement light source SPDs. Thus, it has ten “Load” buttons for the import SPDs, a “Clear SPD Data” button for removing the import data, and a “Plot Spectrum” button to draw the import SPDs in the region II. Besides, the “Weighting” texts behind the “Load” button are used to show the computed mixing ratio of the SPDs.

The region III is used for the user to enter the expected CCT value and the mixing light source number. The “Calculate” button is used to compute the best CRI value after the user set up all requirements. After the calculating, the best CRI value will be shown in the “Max CRI value” text, the chromaticity coordinates position will be drawn in the figure next to it, and the overall mixing SPD will also be plotted in the figure in the region IV.

After the GUI panel has been drawn and the brief functionalities of each region have been described, the interior computations and the details of each block are also needed to be set up. In region I, the default file type is the Microsoft® Excel data sheet. Thus, the user only needs to click the “Load” button and the program will open a new window for the user to select the import files and load them into the database [Fig. 3.8].

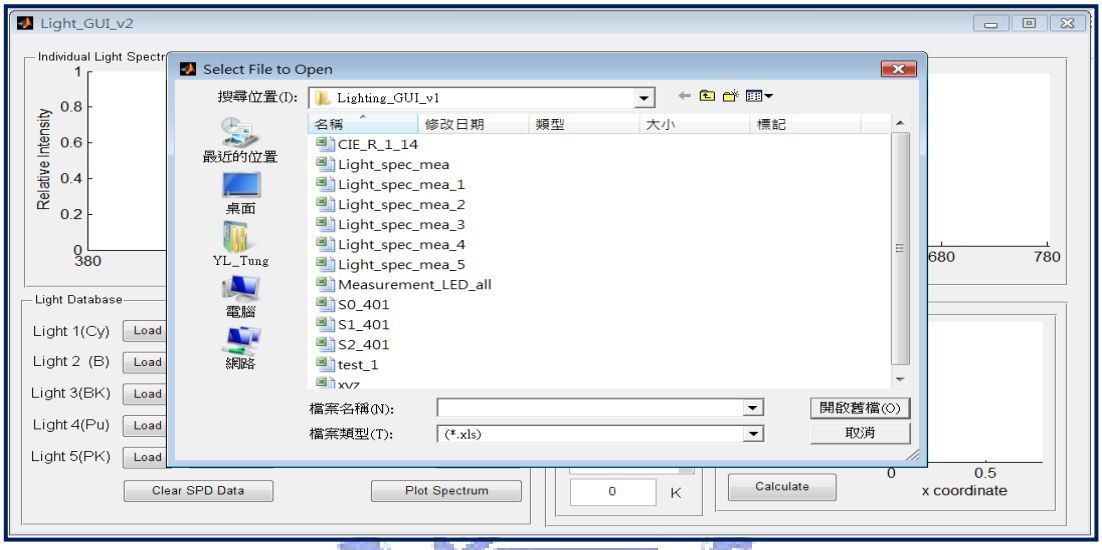

Fig. 3.8 Import file interface

When all files are loaded into the database of the program, the user can push the “Plot Spectrum” button, and the SPDs of the import data will be drawn on the “Import Light Source Spectrum” panel with the line colors describe before their “Load” button [3.9]. Besides, the user only needs to push the “Clear SPD Data” button to eliminate the loading data.

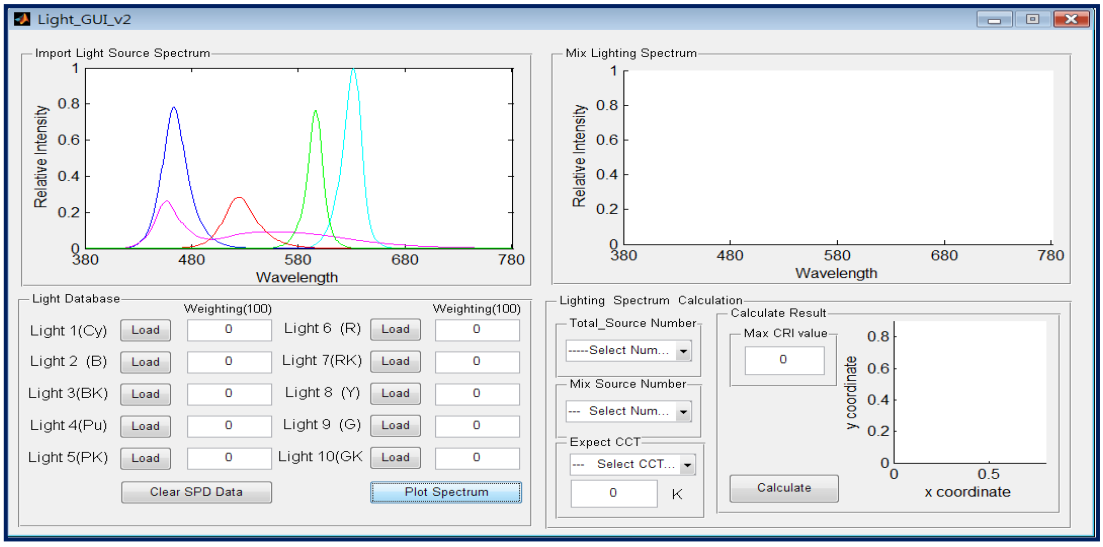

Fig. 3.9 Plot spectrum

After importing basic information about the SPDs, the user can set up the requirements for the calculation on the “Lighting Spectrum Calculation” panel. First of all, the user needs to give the total number of the import SPDs. After that, the program can let the user to choice the light source number in the SPD mixing calculation or to choice the ”Global sol” to receive the maximum CRI value from all possible combinations, and the range of mixing number is from 2 to the total light source number [Fig. 3.10].

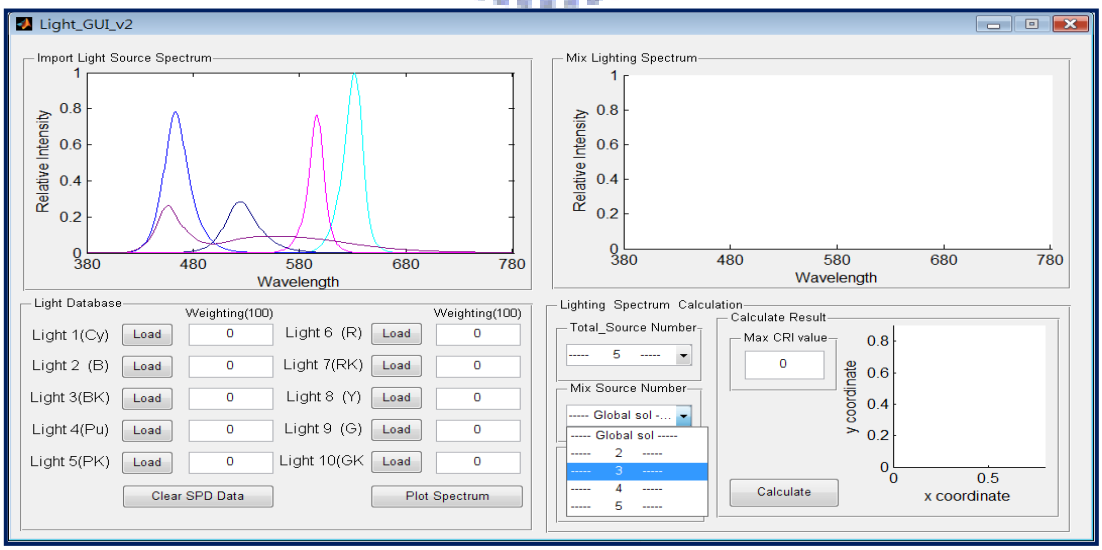

Fig. 3.10 Select mixing number

After selecting the mixing light source number, the user should then select the CCT value at the “Expect CCT” unit, which has four general CCT values and one user input option. When user choices the “Other” option, the user should then enter the CCT value in the text space under the selection menu [Fig. 3.11].

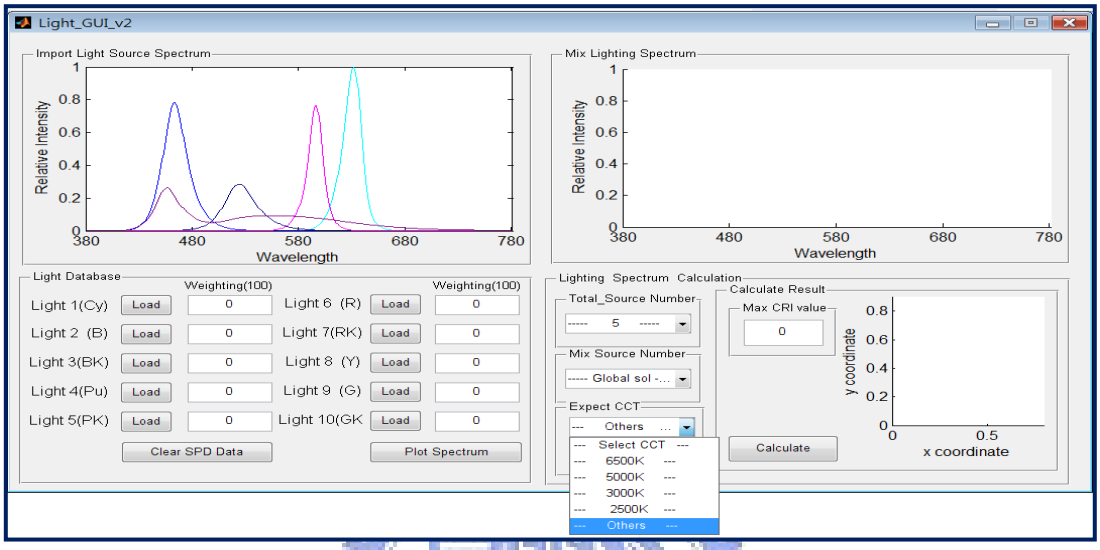

Fig. 3.11 Select CCT value

After finishing all setup, the user only needs to push the “Calculate” button and the program will automatically compute the mixing ratio with max CRI value. The CRI value is then shown at the “Max CRI value” text, and the calculated ratio will display at the “Weighting” texts behind each “Load” button, and the default mixing ratio is set to be 128 levels. Besides, the mixing SPD and the reference illuminance SPD are drawn at “Mix Lighting Spectrum” panel with red and blue color respectively, and the reference position chart is plotted at the right-hand side of the “Calculate Result” panel, the green line shows the monochromatic light locus, red line shows the black body locus, blue line shows the correlated color temperature locus, and the yellow point shows the mixing light chromaticity coordinates [Fig. 3.12].

After all, we demonstrate a GUI program which is easily to use and can help the user to calculate the relative mixing ratio of multi-light sources to fulfill the expected requirements.

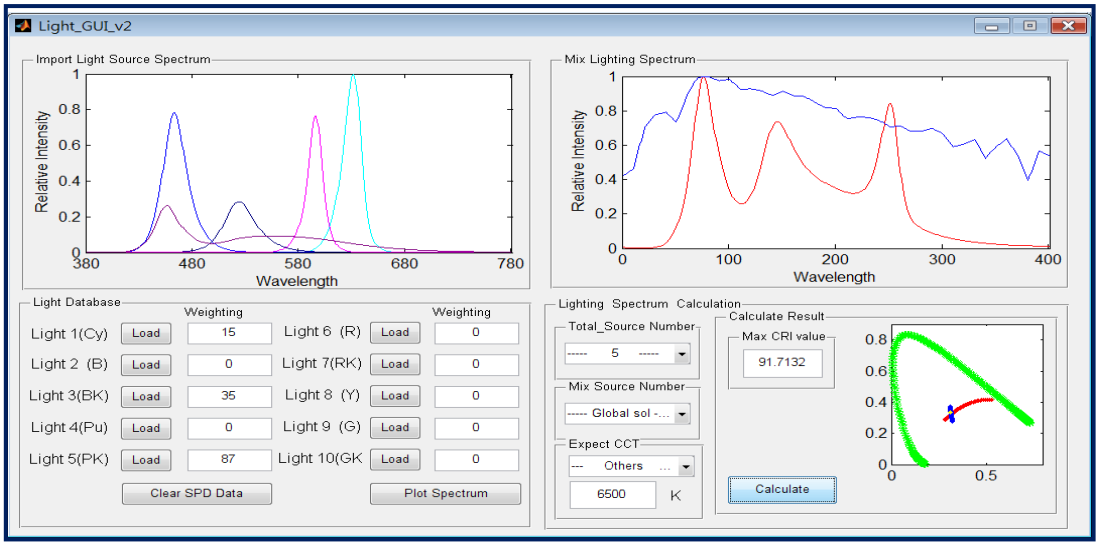

Fig. 3.12 GUI (Example: D65 with three LED sets)

Chapter 4

Experimental Results

In the previous chapter, we have demonstrated a GUI program for mixing light source calculation. Thus, in this chapter, we will use it as a tool to design a LED matrix, and then verify the calculation results.

4.1 Design of LED Matrix

In the beginning of the chapter, we designed the specifications of a LED matrix with tunable CCT value and with acceptable CRI value. Due to the reason that only limited options of primary LEDs are available, we used only four primary color LED lamps and one phosphor white LED lamp.

First of all, we measured three SPDs of each color as the preset database for the simulation. Topcon® SR-UL1R colorimeter was used to measure the SPDs. The results showed that the LEDs have huge intensity variation [Fig. 4.1]. Thus, we used the average SPD for the following simulations.

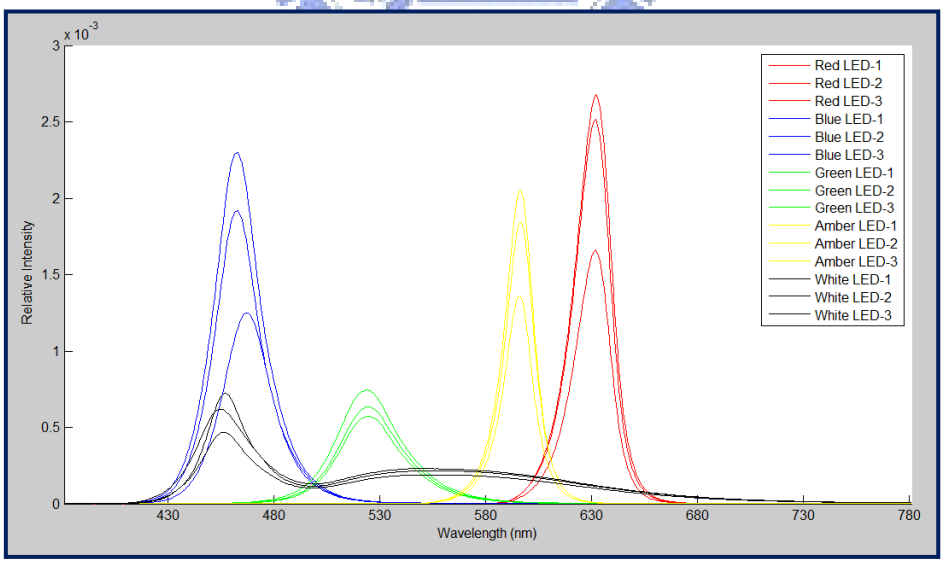

Fig. 4.1 Measurement SPDs

We then imported the average SPDs into the program and simulated the performance under different combinations. The simulation was divided into two segments, Sim I and Sim II. Each segment also includes two sets of intensity ratios,

labeled as part (a) and part (b). The LED sets used in the simulations are shown as below [Table. 4.1].

Sim I	**Part (a)**	1. Blue, green, red, amber, and white LEDs. 2. Preset measured intensity ratios.
	Part (b)	1. Blue, Green, Red, Amber, and white LEDs. 2. Equal intensity ratios.
Sim II	**Part (a)**	1. Blue, green, red, and amber LEDs. 2. Preset measured intensity ratios.
	Part (b)	1. Blue, green, red, and amber LEDs. 2. Equal intensity ratios.

Table 4.1 Settings of the simulations

The difference between Sim I and Sim II is the LED number used. Four primary color LEDs with one phosphor white LED were used in the Sim I, and only four primary LEDs were used in the Sim II. Besides, the simulation of part (a) used the original intensity ratio for simulation, and the part (b) used the equal intensity ratio. The chosen CCT values were 6500K, 5000K, and 2856K. These values stand for reference illuminants D65, D50, and A, respectively.

Five measured primary SPDs used in Sim I part (a) are shown in Fig. 4.2. The CRI values for different CCT values are shown in table 4.2. Besides, the equal intensity SPDs used for the Sim I part (b) are shown in Fig. 4.3. The simulation results are also shown below in table 4.3.

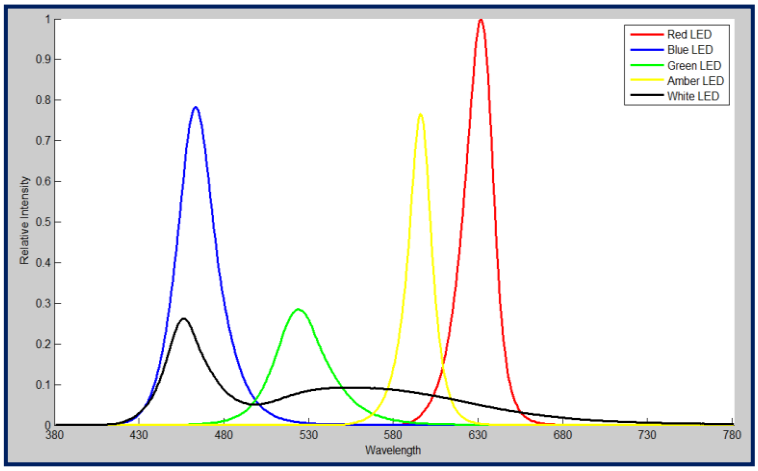

Fig. 4.2 SPDs used in Sim I part (a)

CCT	CRI
6500K	91.71
5000K	91.14
2856K	84.76

Table 4.2 Simulation CRI values of Sim I part (a)

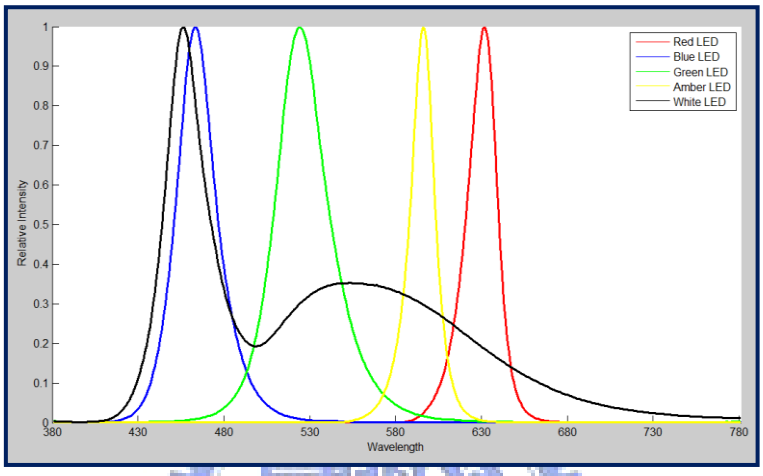

Fig. 4.3 SPDs used in Sim I part (b)

CCT	CRI
6500K	95.17
5000K	94.89
2856K	85.83

Table 4.3 Simulation CRI values of Sim I part (b)

In the next simulation, Sim II, only four primary LEDs were used. The simulation process was the same as the previous one, and the SPDs used are shown in Fig. 4.4 and Fig. 4.5. The corresponding CRI values are shown in table 4.4 and table 4.5, too.

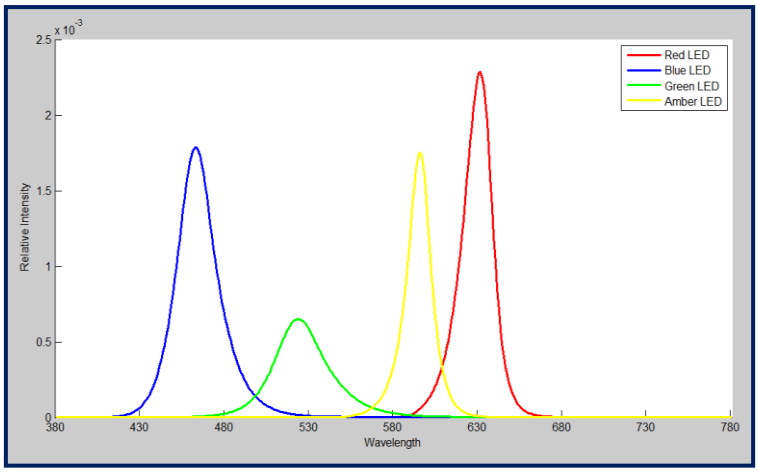

Fig. 4.4 SPDs used in Sim II part (a)

CCT	CRI
6500K	84.59
5000K	87.27
2856K	82.75

Table 4.4 Simulation CRI values of Sim II part (a)

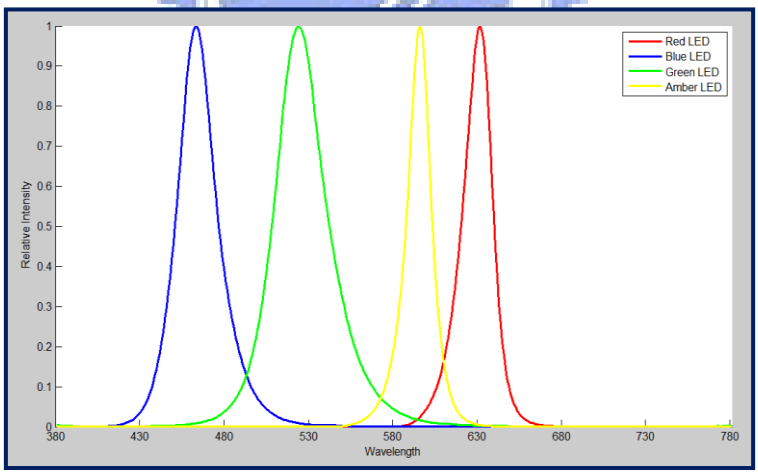

Fig. 4.5 SPDs used for Sim II part (b)

CCT	CRI
6500K	90.07
5000K	88.59
2856K	82.59

Table 4.5 Simulation CRI values of Sim II part (b)

In both simulations, the CRI values are all higher than 80, which is acceptable for general applications. Besides, we found out that the equal intensity SPDs seem to have better CRI values, especially for high CCT values. This is due to the reason that the original green LED we used is not bright enough, thus the mixing SPD is lower than standard illuminant SPD even when the green LED is turned to maximum brightness [Fig. 4.6]. Therefore, we expected to increase the number ratio of the green LED in the matrix.

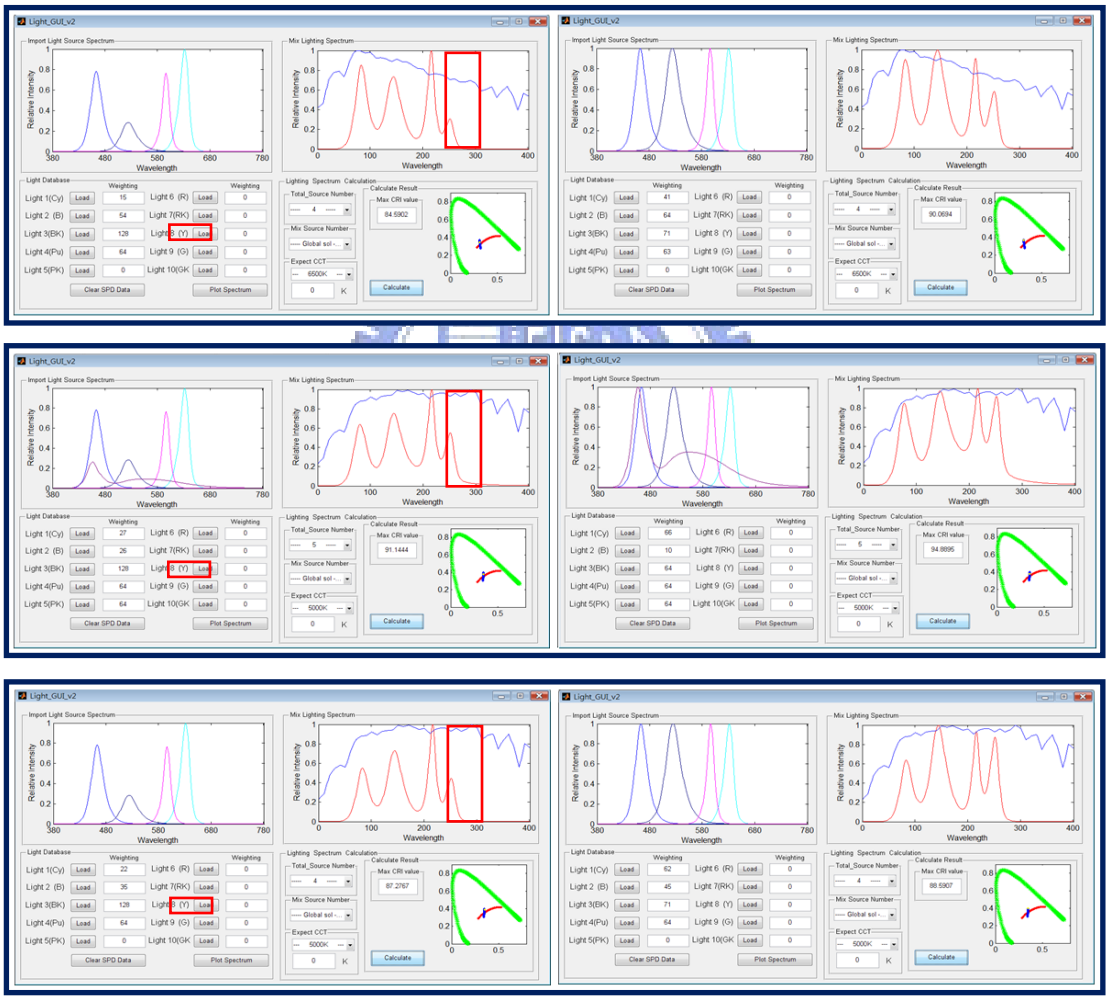

Fig. 4.6 Insufficient of the green LED intensity

In the design of the LED matrix, we divided the whole LED clusters into sixty-four sub-blocks. Each sub-block was designed to have the primary LED number ratio 1:3:1:1:3 with the color blue, green, amber, red, and white respectively. This ratio came from the previous simulation results. The specifications of the LEDs we

adopted are shown in Table 4.6, and the overall arrangement of the LED matrix is also shown below [Fig. 4.7].

Wavelength	465	525	589	623	White
Intensity (mcd)	2000	7000	4000	5000	8700
Viewing Angle($\Theta_{1/2}$)	30°	30°	30°	30°	30°
Forward Voltage(V)	3.4	3.4	2	2	3.4

Table 4.6 Specifications of the LEDs

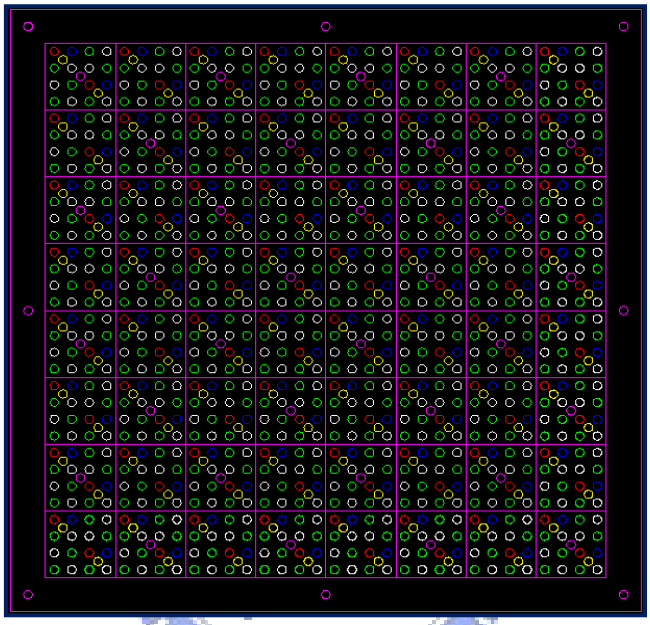

Fig. 4.7 Layout design of LED matrix

In the control part of the matrix, the system was designed to have 128 gray levels for each color LED. PWM is the most general method for the LED dimming, and only occurs small spectrum deviation during the modulation [18]. Thus, we adopted PWM for our intensity modulation. The general specification of the matrix is shown below in table 4.7 and the overall LED matrix system was developed by the Green Resource Enterprise Cooperation [Fig.4.8].

Parameters	Value
Matrix size	32cm x 32 cm (8 unit x 8 unit)
Unit size	4cm x 4cm
LED number	Total : 1152 Blue : 128 → 1 Green : 384 → 3 Amber: 128 → 1 Red : 128 → 1 White : 384 → 3
Gray level	128

Table 4.7 Specifications of LED matrix

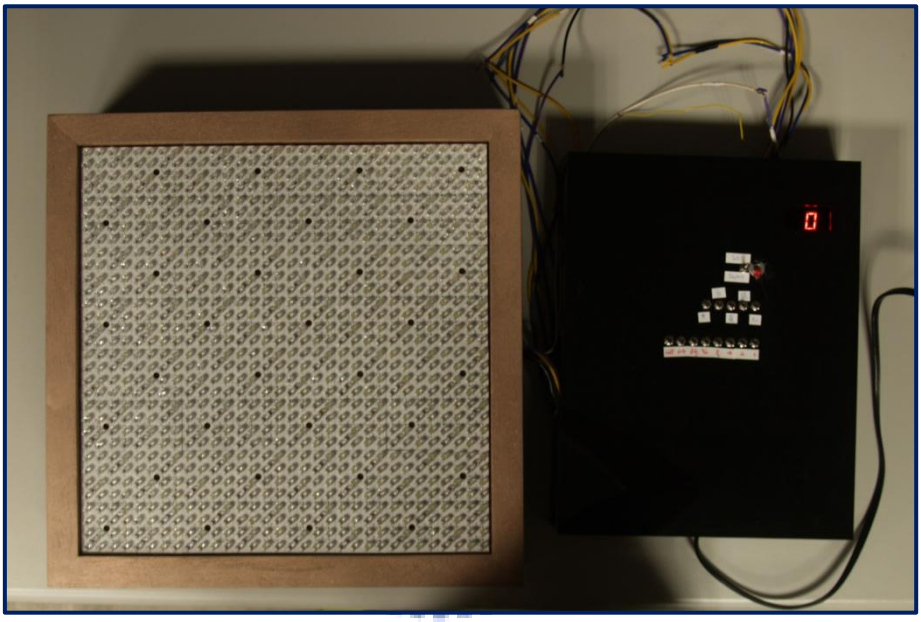

Fig. 4.8 Tunable LED matrix

4.2 Measurement Results

After the tunable LED matrix had been constructed, we first confirmed the control property of the matrix. The oscilloscope DSO6034A, Agilent Technologies® , was used to monitor the control signal of the gray levels [Fig. 4.9, Fig. 4.10]. The frame time of the full on LED is 6.66ms, and reduce between 0.04ms and 0.06ms for each decreasing gray level. The measurement result of each color LED is shown in table 4.8. However, the time variation of each gray level is not stable, and this might cause some deviation of the mixing SPD.

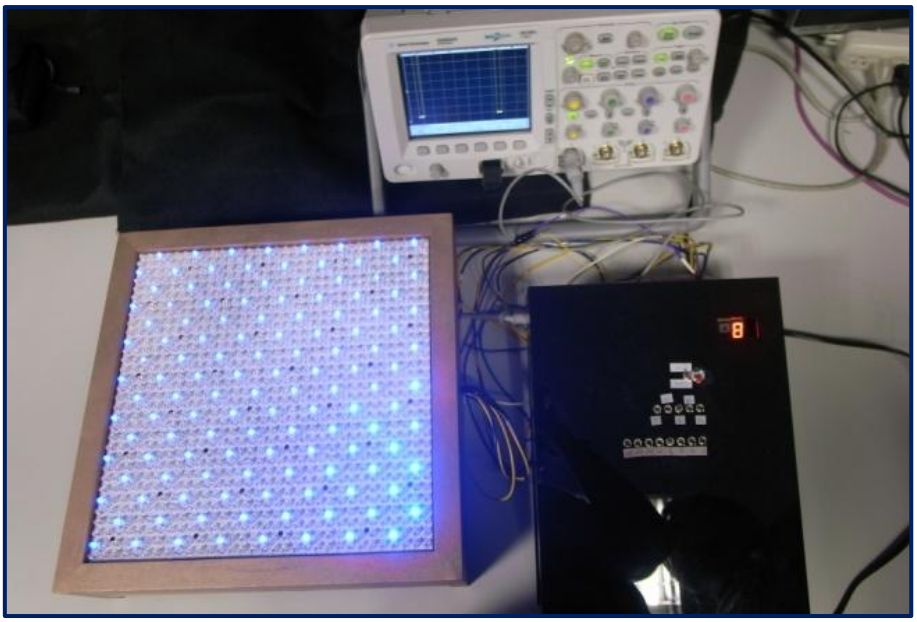

Fig. 4.9 Verification of the PWM method

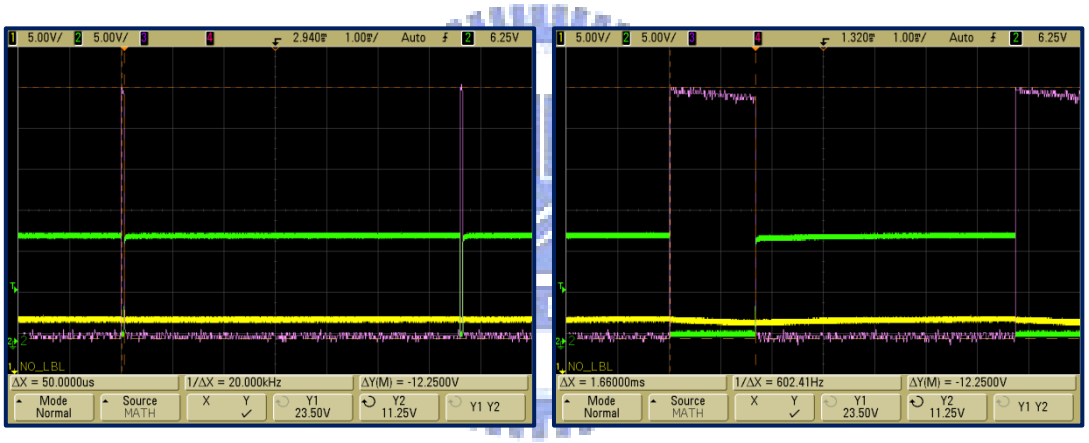

(a.) PWM signal with gray level 1 (b.) PWM signal with gray level 32

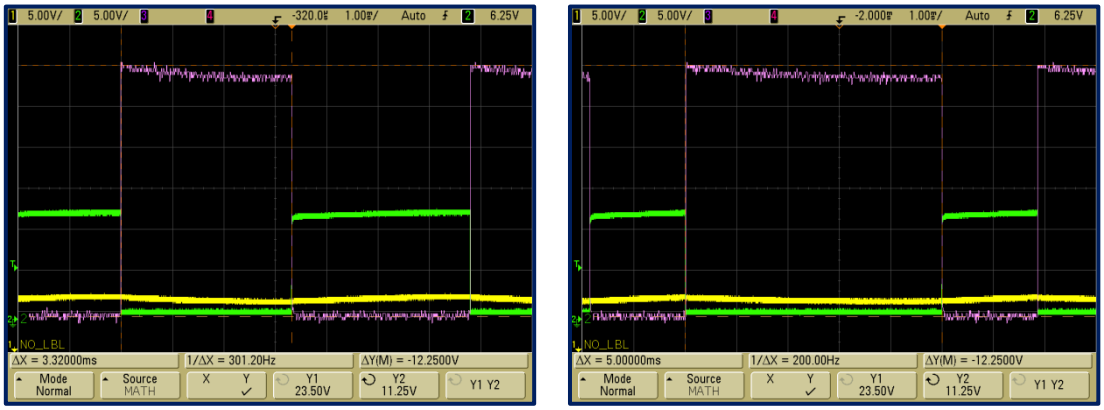

(c.) PWM signal with gray level 64 (d.) PWM signal with gray level 96

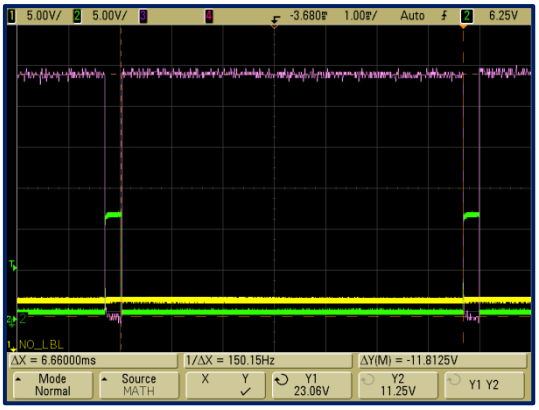

(e.) PWM signal with gray level 128

Fig. 4.10 Red LED PWM signals with different gray levels

Gray Level\Color(ms)	Blue	Green	Red	White	Amber
1	0.05	0.06	0.06	0.05	0.06
32	1.66	1.67	1.66	1.66	1.66
64	3.32	3.32	3.34	3.34	3.32
96	5	5	5	5	5
128	6.66	6.66	6.66	6.66	6.66

Table 4.8 The pulse width time of LEDs under different gray levels

Then, the SPDs of each LED with the highest gray level were measured by the colorimeter [Fig. 4.11]. As show in the measurement results, the intensity of the green light LED is enhanced. Thus, the blue, green, red, and white LEDs have the comparable intensity as we expect. However, the intensity of the amber LED is half lower than the others, which is caused by the dramatic difference SPD between the previous measured LED samples and the practical matrix LEDs, and this might decrease the CRI performance of the matrix.

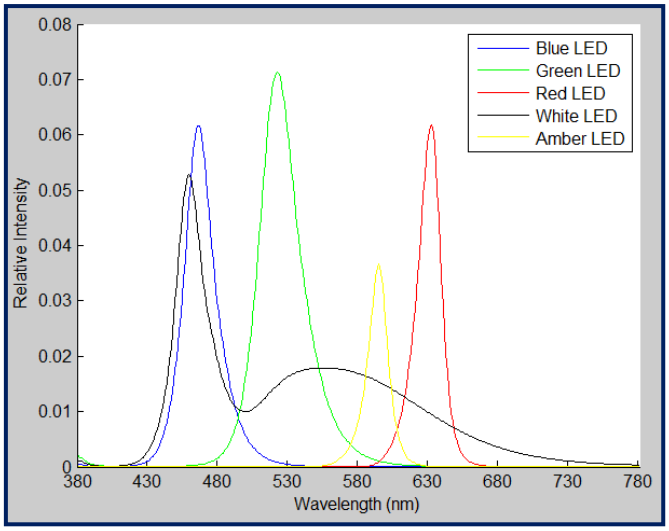

Fig. 4.11 SPDs of the LED matrix

After receiving the SPDs of the LED matrix, we used the developed GUI interface to calculate the matrix mixing ratio with CCT values 6500K, 5000K, and 2856K. The simulation also took two conditions, SET I and SET II, into account. In SET I, four primary LEDs and one phosphor white LED were used. And only four primary LEDs were used in SET II calculation. The computation results of each case are shown in table 4.9 (a) and table 4.9 (b), respectively.

SET I	With white LED		
	6500K	5000K	2856K
Blue	0	0	0
Green	27	43	22
Red	45	63	63
White	95	79	15
Amber	0	64	67
CRI value	94.31	95.94	84.27

(a) Mixing ratios of SET I

SET II	Without white LED		
	D65	D50	A
Blue	64	45	7
Green	61	59	27
Red	66	85	60
Amber	64	65	77
CRI value	81.81	74.34	80.29

(b) Mixing ratios of SET II

Table 4.9 Simulation mixing ratios

We then used the colorimeter to measure the SPD of the matrix [Fig. 4.12]. We adopted $0^o/45^o$ measurement setup, which means that the light illuminate from the normal side of the white plate, and the colorimeter measured the reflection SPD from the 45^o degree position. The white plate is a small disc made by $BaSO_4$, which has smooth reflection spectrum over the visible range, and is usually used to measure the light source SPD. The measurement SPDs and the GUI SPDs are shown in Fig. 4.13 and the compare of the CCT and CRI values are shown in the Table 4.10.

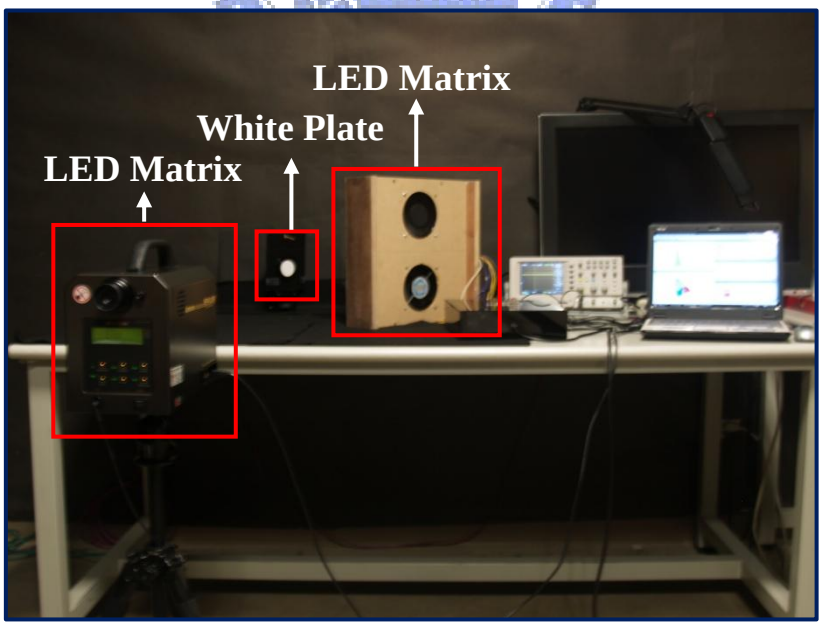

Fig. 4.12 Experimental setup of the spectrum measurement

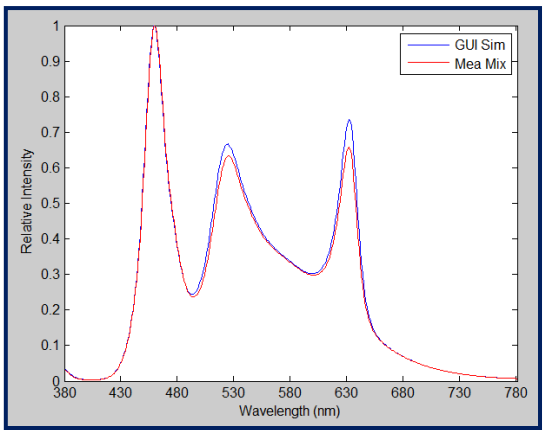

(a.) D65 with white LED

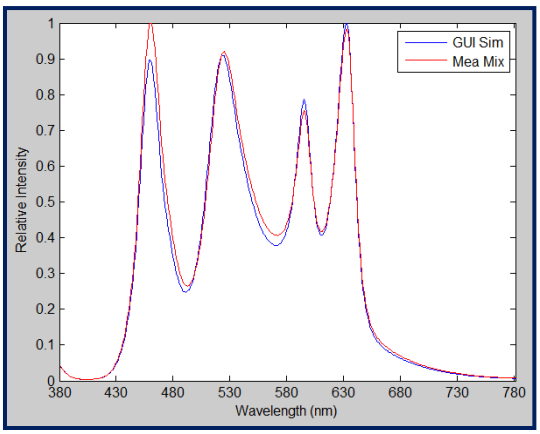

(b.) D50 with white LED

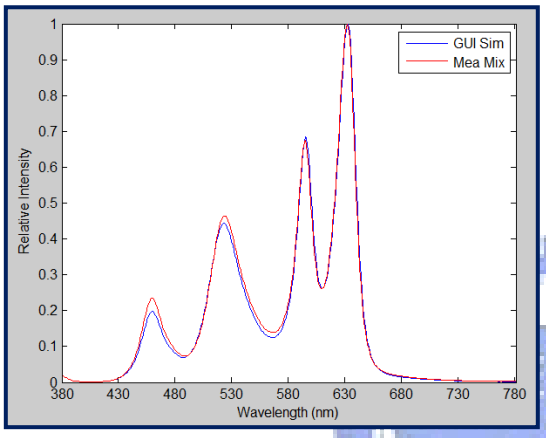

(c.) A with white LED

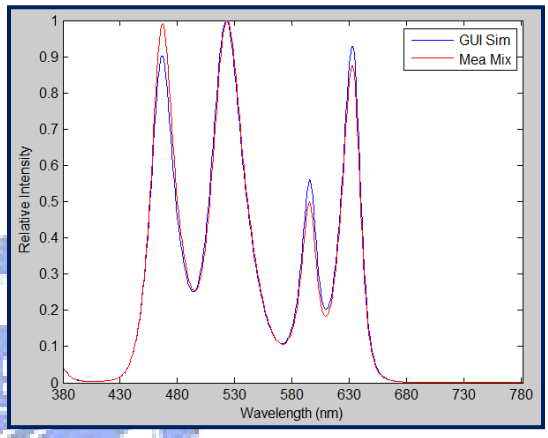

(d.) D65 without white LED

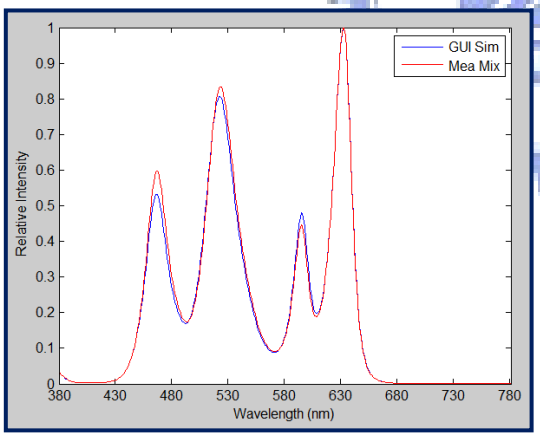

(e.) D50 without white LED

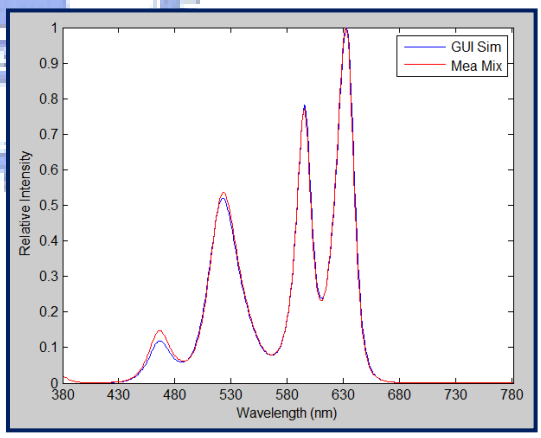

(f.) A without white LED

Fig. 4.13 GUI SPDs and Measurement SPDs

SET I	With white LED		
	6500K	5000K	2856K
CCT (GUI Simulation)	6529	5021	2859
CCT (Measurement)	6723	5252	2995
CRI (GUI Simulation)	94.31	95.94	84.27
CRI (Measurement)	94.68	96.18	86.15

(a.) SPDs with white LED

SET II	Without white LED		
	6500K	5000K	2856K
CCT (GUI Simulation)	6513	5012	2856
CCT (Measurement)	7128	5293	2943
CRI (GUI Simulation)	81.81	74.34	80.29
CRI (Measurement)	83.47	75.12	81.33

(b.) SPDs without white LED

Table 4.10 Compare of the CCT and CRI values

4.3 Discussions and Modifications

From the experiment results, the measured SPDs are obviously deviating from the simulation ones, and the CCT values of the measurements are not confirmed with the simulation values. Thus, we need more detailed measurements to analysis the system. First of all, we measured the SPDs of each LED with 4 gray levels separation. From the results, we found out that the SPDs are increasing linearly over the wavelengths at low gray levels, but deforming at high levels [Fig. 4.14]. The deformations were occurred from one edge to the half of the SPD, and the other half

of the SPD seemed to increase linearly. Thus, the SPD profile might change when LED is operating at different gray levels. However, only slight difference was observed from the comparison of the measured SPDs and the simulation ones, [Fig. 4.15].

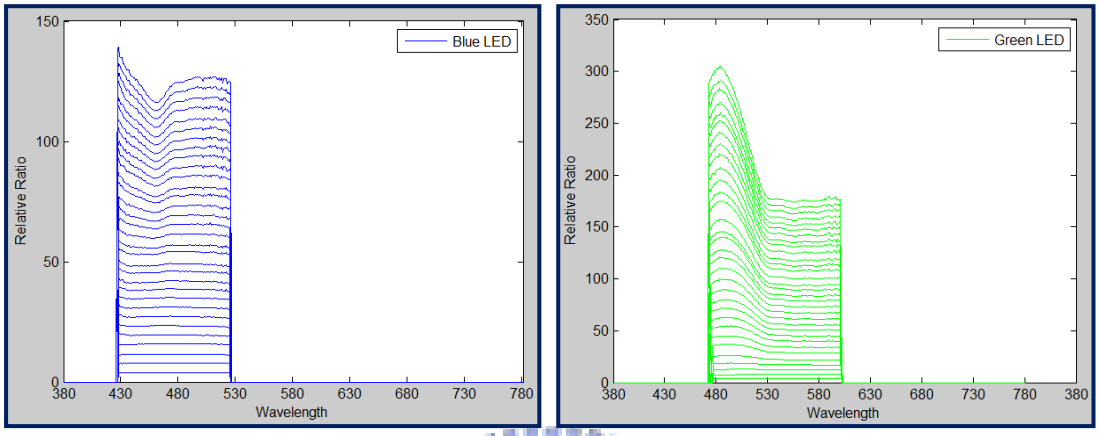

(a.) SPD variations of blue LED (b.) SPD variations of green LED

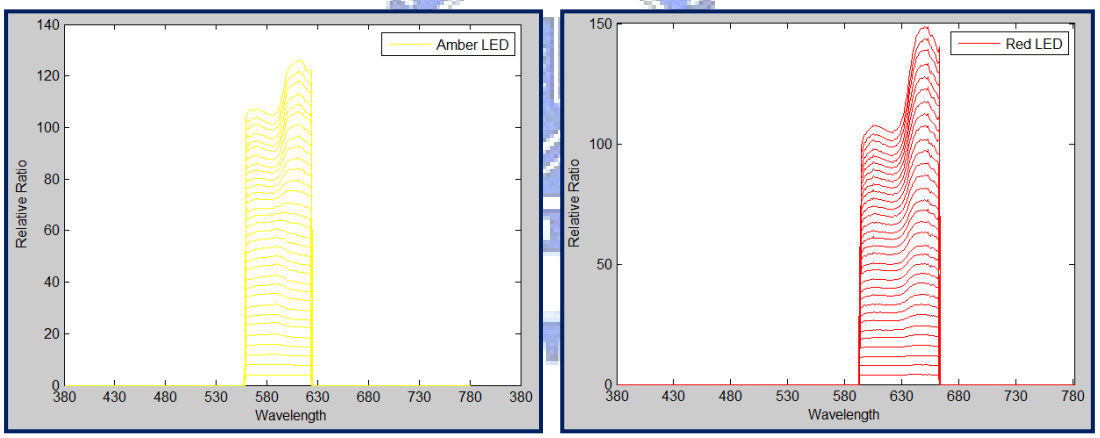

(c.) SPD variations of amber LED (d.) SPD variations of red LED

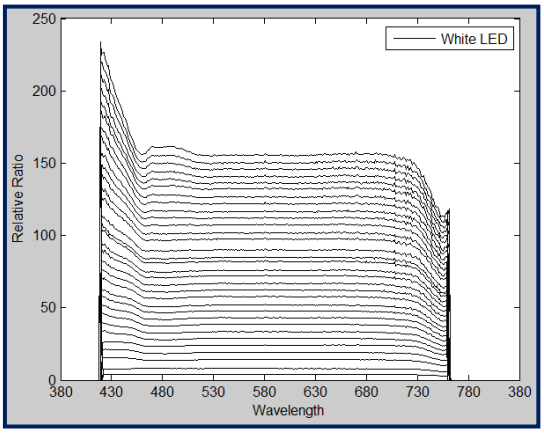

(e.) SPD variations of white LED

Fig. 4.14 Variation ratios of different LED SPDs

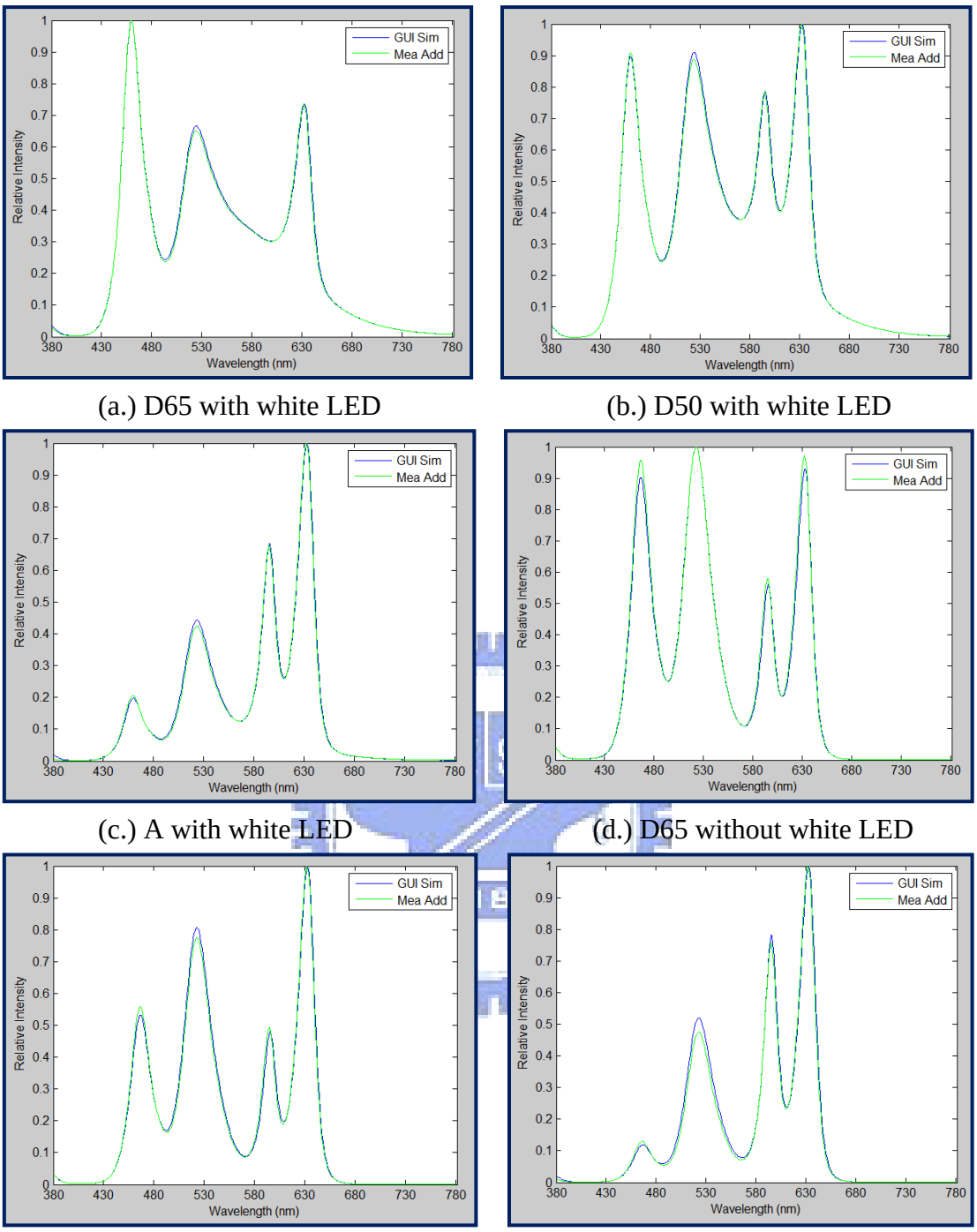

(a.) D65 with white LED (b.) D50 with white LED

(c.) A with white LED (d.) D65 without white LED

(e.) D50 without white LED (f.) A without white LED

Fig. 4.15 GUI simulation SPDs and Measurement primary LED addition SPDs

Thus, the deformation of the LED profile is not the primary issue for the variations of the measured SPDs and the simulation ones. By more detailed observation of the matrix operations, we than found out that the addition of primary LED SPDs were not actually matched with the mixing SPDs. The oscilloscope showed that the PWM signal is deforming when more than one kind of LED is turned

on, here we show the SET I 6500K measurement results in Fig. 4.16. From the measurement results, the duty cycle of the control signal is increasing and the operating voltage is descending for the mixing SPDs.

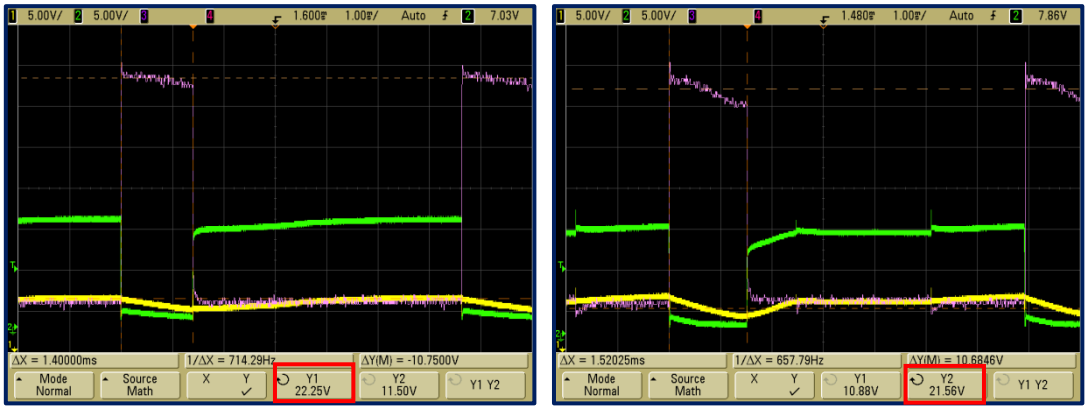

(a.) PWM signal of primary green LED (b.) PWM signal of mixing green LED

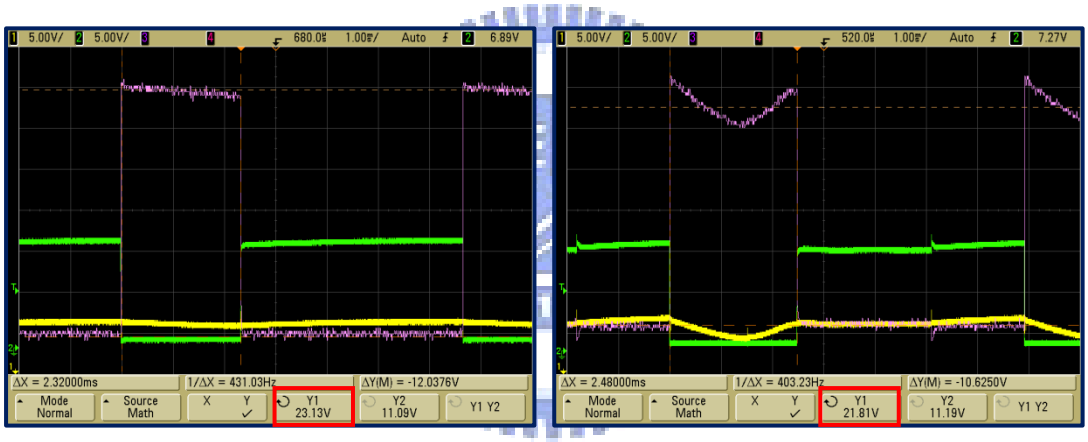

(c.) PWM signal of primary red LED (d.) PWM signal of mixing red LED

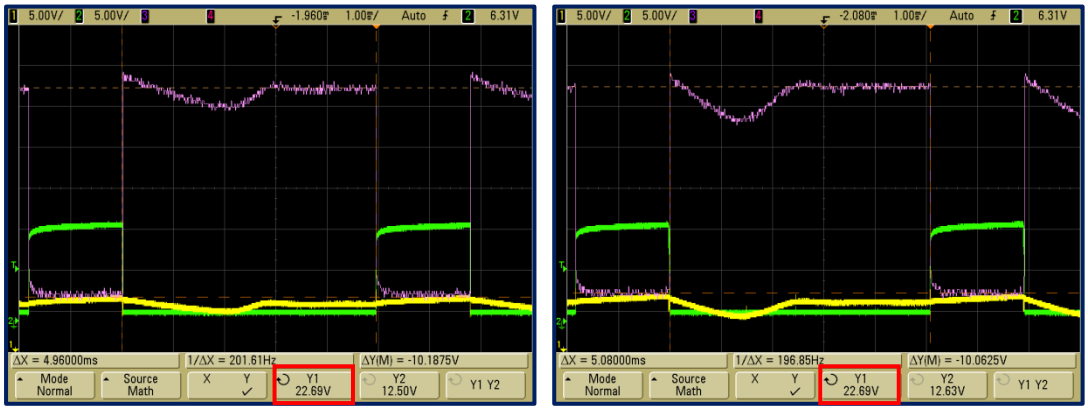

(c.) PWM signal of primary white LED (d.) PWM signal of mixing white LED

Fig. 4.16 Measurement results of SET I 6500K PWM signals

After that, we use the multimeters to monitor the operating voltage and the current. We then use the measured result to modify the simulation results. By the mechanism of the LED, the emitting radiance is proportional to the operating power, which can be simply written as equation 4.1, where P_{ave} is the time average power, V_{ave} is the time average voltage, and I_{ave} is the time average current.

$$P_{Ave} = V_{Ave} \times I_{Ave} \qquad \text{(Eq. 4.1)}$$

Therefore, we included the operating power as a factor to correct the simulation process used for synthesizing mixing SPDs. The corrected SPDs are really confirmed the measured ones [Fig. 4.17]. The CCT values of the two SPDs are also almost equal [Table 4.11]. Thus, we believed that the variations between the original simulation SPDs and the measured SPDs are caused by the system circuit crosstalk, and can be revised by including adequate correcting factor into our simulation process.

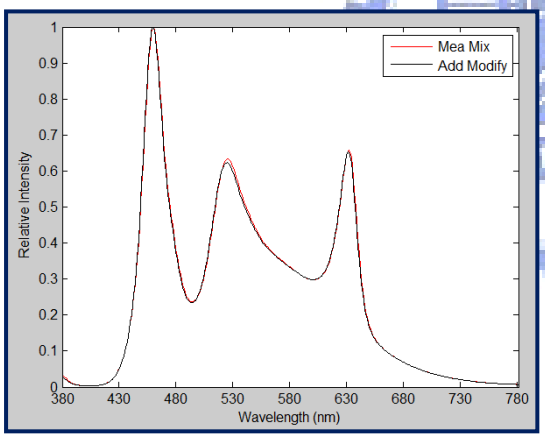

(a.) D65 with white LED

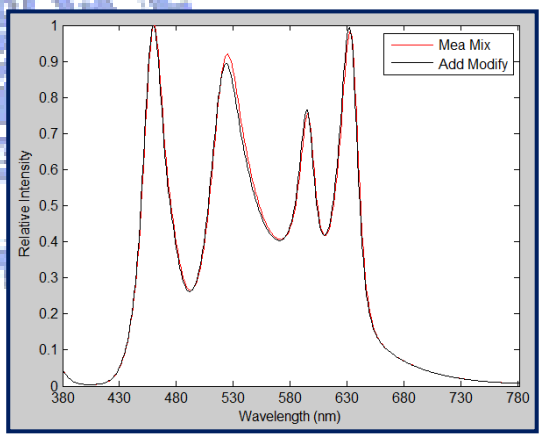

(b.) D50 with white LED

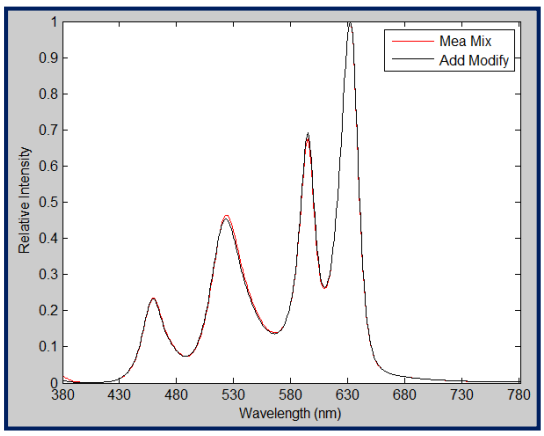

(c.) A with white LED

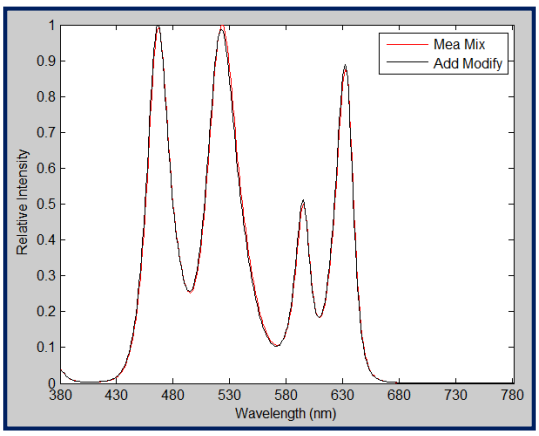

(d.) D65 without white LED

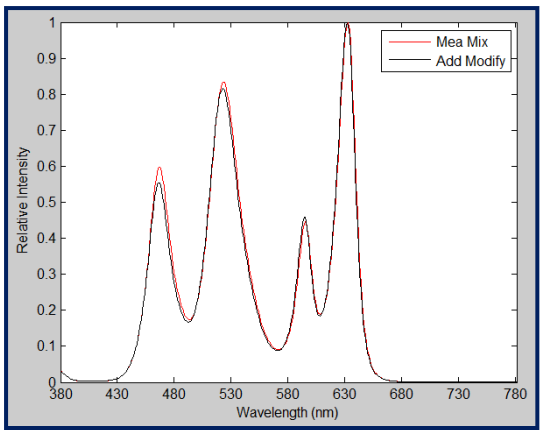

(e.) D50 without white LED

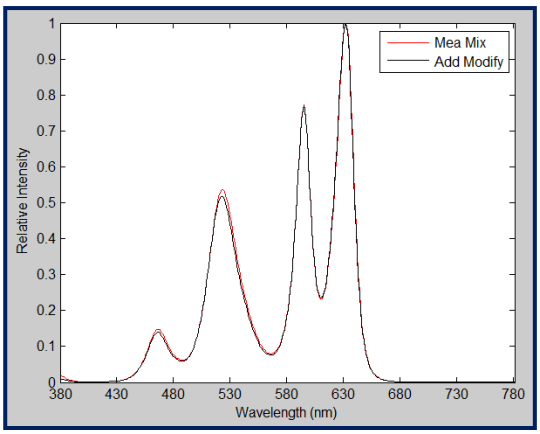

(f.) A without white LED

Fig. 4.17 Modified addition SPDs and measurement SPDs

	SET I			SET II		
	6500K	5000K	2856K	6500K	5000K	2856K
CCT (Measured)	6723	5252	2995	7128	5293	2943
CCT (Corrected from primary addition)	6728	5197	2936	7171	5134	2863

Table 4.11 Compare of the CCT values

Chapter 5

Conclusions and Future Works

In this thesis, we have successfully accomplished a GUI platform for multi-color LED mixing calculation. The simulation result is well verified by a LED matrix with tunable CCT value and high CRI value. Although the crosstalk is occurred by the control circuit, the platform still can modify the simulation result and expect the synchronized mixing SPD. Thus, this GUI platform will be a powerful tool for the further LED lighting study.

In the future, the program is able to expand or replace some new elements. For example, the new generation light source qualification factor, color quality scale (CQS), which is developed by Yoshi Ohno and Wendy Davis at national institute of standard and technology (NIST), USA [19]. This factor is established to modify the CRI value in order to achieve better correlations between the human feeling and the evaluating scores.

CQS pronounced 15 high saturation color chips to replace the 8 low saturation samples used in CRI [Fig. 5.1]. The samples are selected to span around the entire hue circle and are expected to have better representation of the practical object colors. Besides, the more uniform and advanced color space, CIE 1976 L*a*b* is adopted than the original 1964 W*U*V* color space. Current research shows that only decrease in chroma will have negative effects. Thus, CQS also takes this into consideration, and maintain the evaluating score when the chroma is increased. This is different than the CRI evaluation, which will decrease the score for any color deviation. Furthermore, CQS takes root-mean-square (RMS) than the traditional arithmetic mean to evaluate the overall score. This is used to emphasize the performance of each sample.

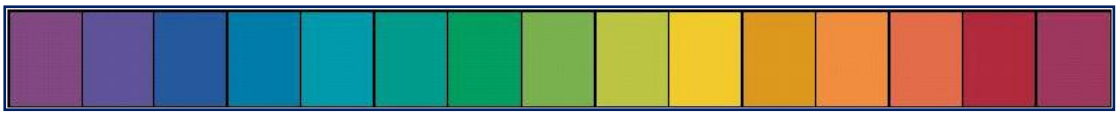

Fig. 5.1 Color chips used in CQS

However, some parts of this new scale are under developing, such as new human adaptation model. Besides, the practical human experiment results are not published, and the CIE still not accepts it as the global standard. Therefore, we still took the CRI into our consideration until the accurate calculating process is available.

Besides the modification of the GUI platform, some LED lighting issues can also be discussed in the future. Some research had done to discuss the impact of the working performance under different lighting intensity. Beutell is the first one who attempted to announce a model for specifying the necessary illuminance for different task [6]. And the idea was exploited by Weston who developed it into one of the most widely used methods of investigating the effects of lighting and work [6]. Weston devised a very simple task which was largely visual and in which the critical detail was easy to identify and measure. The task is well known as the Landolt ring chart [Fig. 5.2]. Thus, the tester can analysis the experimental scores to evaluate the lighting performance.

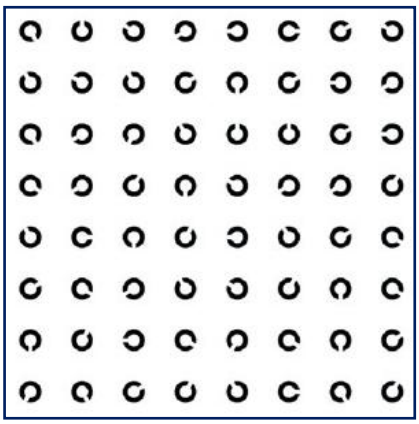

Fig. 5.2 Landolt ring chart

However, only luminance issue is considered in the past experiment. Nowadays, the LED produces a chance to receive many different spectrums with the same chromaticity. This phenomenon is called the metameric spectrum in color science. As the previous studies had done on the working performance with different lighting intensity, we are more interesting in the influence of the metameric spectrum to the working performance, or the color contrast to the working performance. Although the parameters, such as CRI value or CQS, can describe the color performance of the light source, they have no link between these index values and the human working performance. Thus, our GUI platform can be used to produce different SPD light sources with the same CCT value, and then two environments that fulfilled the traditional lighting requirements with different SPDs can be constructed. Then, we can compare the working performance under the different spectrum condition and find out more LED lighting properties.

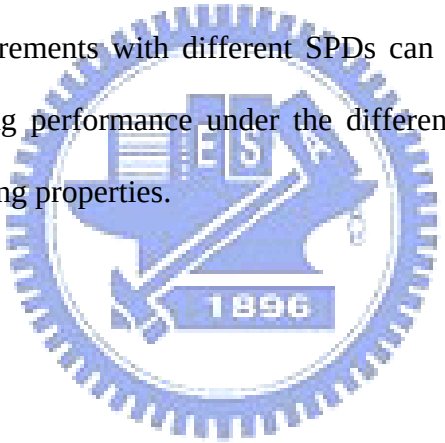

Reference

[1] *"Global Optoelectronics Industry Market Report and Forecast"*, OIDA, 2007

[2] Daniel A. Steigerwald, Jerome C. Bhat, Dave Collins, Robert M. Fletcher, Mari Ochiai Holcomb, Michael J. Ludowise, Paul S. Martin, Serge L. Rudaz, "Illumination With Solid State Lighting Technology," *IEEE Journal On Selected Topic in Quantum Electronics*, Vol. 8, No. 2, pp.310-320, 2002.

[3] Advanced Lighting Guidelines Project Team, "Advanced Lighting Guidelines," New Buildings Institute, Inc, 2003.

[4] "Lighting Applications Guideline for LEDs," Lighting Research Center, Rensselaer Polytechnic Institute, 2002.

[5] http://www.philipslumileds.com/technology/lumenmaintenance.cfm

[6] P. R. Boyce ,"Human Factors in Lighting", Applied Science Publishers Ltd, England, 1981.

[7] Jennifer A. Veitch, Guy R. Newsham, "Determinants of Lighting Quality I: State of the Science", *Journal of the Illuminating Engineering Society*, Winter, pp. 92-106, 1998.

[8] Jennifer A. Veitch, "Determinants of Lighting Quality II: Research and Recommendations", Lighting Research & Recommendations, National Research Council of Canada, 1996.

[9] Neil Holger White Eklund, "Multiobjective Visible Spectrum Optimization: A Genetic Algorithm Approach", Ph. D Thesis, Rensselaer Polytechnic Institute, 2002.

[10] A. Zukauskas, R. Vaicekauskas, F. Ivanauskas, R. Gaska, M. S. Shur, "Optimization of White Polychromatic Semiconductor Lamps", *Applied Physics Letters*, Vol. 80, pp. 234-236, 2002.

[11] R. Gaska, A. Zukauskas, M. S. Shur, M. Asif Khan, "Progress in III-Nitride Based White Light Sources", *Solid State Lighting II*, Proc. SPIE, Vol. 4776, pp.82-96, 2002.

[12] A. Zukauskas, R. Vaicekauskas, F. Ivanauskas, H. Vaitkevicius, M. S. Shur, "Spectral Optimization of Phosphor-conversion Light-emitting Diodes for Ultimate Color Rendering", *Applied Physics Letters*, Vol. 93, 05115, 2008.

[13] A. Zukauskas, R. Vaicekauskas, F. Ivanauskas, H. Vaitkevicius, M. S. Shur, "Rendering a Color Palette by Light-emitting Diodes", *Applied Physics Letters*, Vol. 93, 021109, 2008.

[14] Noboru Ohta, Alan R. Robertson, "Colorimetry," John Wiley & Sons Ltd, England, 2005.

[15] Commission Internationale de l'Éclairage: Method of measuring and specifying colour rendering properties of light sources. CIE Central Bureau CIE 13.2-1974.

[16] "Lighting Applications Guideline for LEDs", Lighting Research Center, Rensselaer Polytechnic Institute, 2002.

[17] Yoshi Ohno, "Color Rendering and Luminous Efficacy of White LED Spectra", *Fourth International Conference on Solid State Lighting*, Proc. SPIE, Vol. 5530, pp. 88-98, 2004.

[18] B. Ackermann, V. Schulz, C. Martiny, A. Hilgers, X. Zhu, "Control of LEDs", *Industry Applications Conference*, Conference Record of the 2006 IEEE, Vol. 5, pp. 2608-2615, 2006.

[19] Wendy Davis, Yoshi Ohno, "Development of a Color Quality Scale", National Institute of Standards and Technology, 2006.